RESEARCH REPORT EERL 6

T. PARKS

Design and Construction of a Matched Filter

April 1964
TR No. 79

Contract No. DA36-039-AMC-00034(E)

ystem Theory

2

ELECTRICAL ENGINEERING RESEARCH LABORATORY

CORNELL UNIVERSITY
Ithaca, New York

RESEARCH REPORT EERL 6

DESIGN AND CONSTRUCTION OF A MATCHED FILTER

T. Parks

SYSTEM THEORY RESEARCH

Technical Report No. 79 April 1964

Published under U. S. Signal Corps Contract No. DA36-039-AMC-00034(E)
U. S. Army Signal Research and Development Laboratory, Fort Monmouth, N. J.

ACKNOWLEDGMENTS

The author wishes to thank Dr. H. W. Schüssler for his guidance as thesis advisor; also, Prof. N. DeClaris and Prof. J. S. Thorp, for their encouragement and valuable discussions.

Financial support from the Signal Corps made this study possible.

CONTENTS

LIST OF ILLUSTRATIONS

ABSTRACT

This research concerned the design, construction and evaluation of a laboratory model of a wide-band filter matched to a seven-pulse code. A modified link structure with two grid lines provided for both positive and negative coefficients. The grid and plate lines, designed for maximally flat delay, were constructed by cascading constant-resistance all-pass networks, based on the unbalanced lattice. The measured ratio of central to side peaks was about 80 per cent of the theoretical value.

I. INTRODUCTION

The idea of a matched filter originated in studies of maximizing the signal-to-noise ratio at the output of a receiver. It has been shown[1, 2] that if a wave form $f(t)$ consisting of a signal $s(t)$ plus white noise $n(t)$ is passed through a filter whose impulse response $h(t)$ is the time inverse of the signal $s(t)$, the ratio of peak signal to rms noise is maximized. A matched filter has an impulse response of $h(t) = s(-t + T)$. The matched filter output has the best possible ratio of peak signal/rms noise = R. This ratio R is proportional to the energy of the signal $s(t)$ and the power density of the noise $n(t)$. It does not depend on the shape of the wave form $s(t)$.

In many applications, the system used to generate $s(t)$ is peak power-limited. The amplitude of $s(t)$ is limited to some maximum which, for convenience, is normalized to one. In this case, the energy of $s(t)$ may be increased by lengthening the pulse $s(t)$.

Figure 1a shows a pulse $s(t)$ of 1-v amplitude and 1-sec duration appearing across a 1-ohm load resistor. A rectangular pulse is used because it contains the maximum energy when the generator is peak power-limited. The energy contained in $s(t)$ is equal to its area of 1 watt-second = 1 joule. The matched filter for this $s(t)$ has an impulse response $h_1(t) = s(-t + 1)$ (see Figure 1b). The output $g(t)$ is simply $s_1(t)$ convolved with $h_1(t)$, i.e.

$$g(t) = \int_{-\infty}^{\infty} s(\tau)\, h_1(t - \tau)\, d\tau \quad , \tag{1}$$

as shown in Figure 1c.

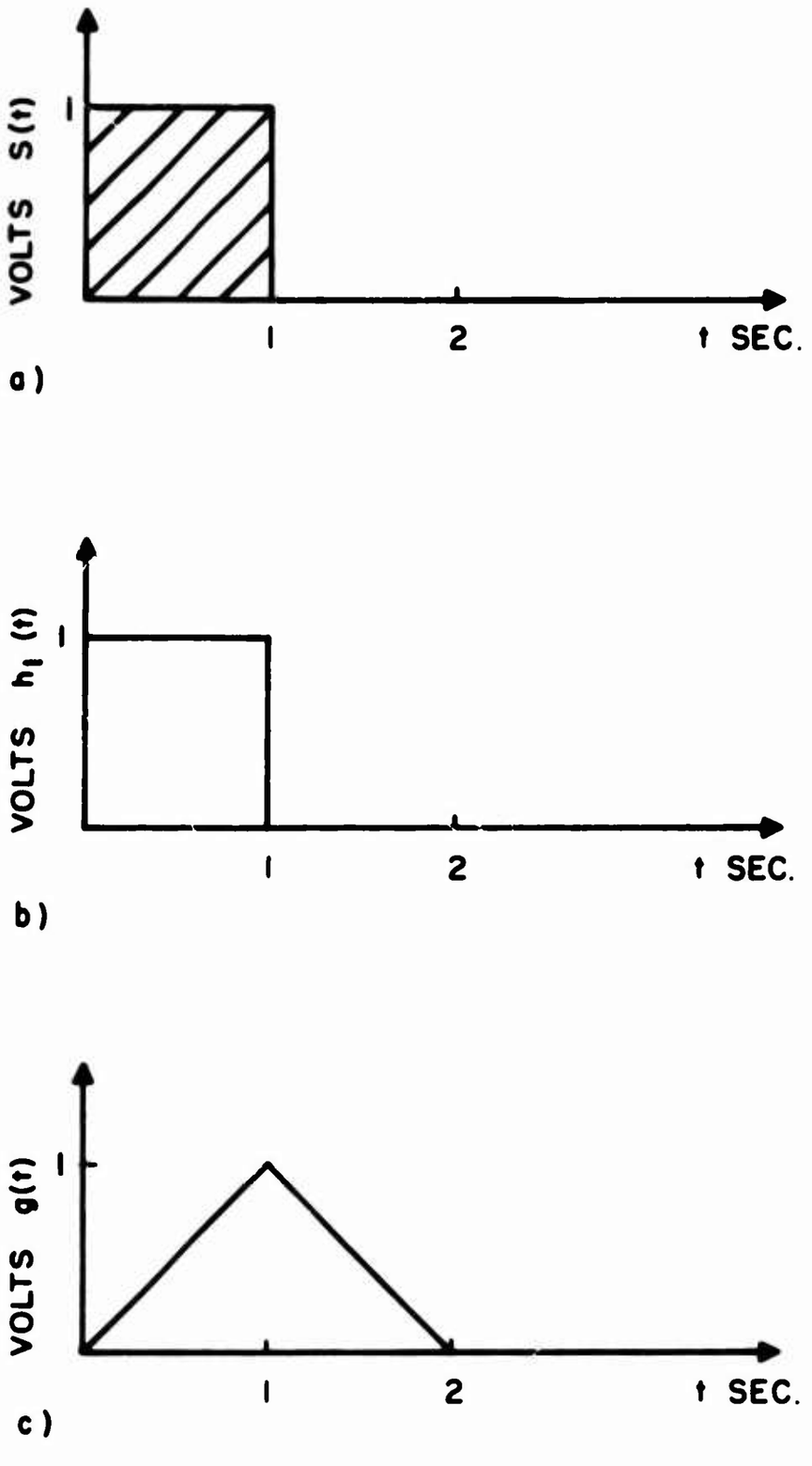

FIGURE 1. Example of Matched Filter, a) Input Signal, b) Impulse Response, c) Output Signal.

If the energy of $s_1(t)$ is increased to 7 joules by lengthening the pulse to 7-sec duration, the peak output voltage is also increased by a factor of seven (Figure 2). While the peak of the output signal is increased by lengthening $s(t)$, the duration of the output signal is also increased. It is not as easy to determine when the peak of $s_7(t)$ occurs. In other words, resolution with $s_1(t)$ is better than with $s_7(t)$.

Pulse-coding[2] offers a method for changing the shape of $s(t)$ so that its energy may be increased while retaining the desired resolution (Figure 3). The peak of the output signal $g_7^1(t)$ in Figure 3 is the same as $g_7(t)$ (Figure 2), but the output is the same width as $g_1(t)$ (Figure 1).

Networks which produce signals like $s_7^1(t)$ (generators) and have an impulse response like $h_7^1(t)$ (matched filters) have been constructed[3] using tapped delay-lines and resistor-summing networks (Figure 4). The signal at the m^{th} tap of the delay line is $a_m h(t - nT)$, where a_m is the gain or weight associated with the m^{th} tap, $h(t)$ is the impulse response of the prefilter or pulse-shaping network, and τ is the delay between taps on the delay line. The output of the coded-pulse generator is

$$s_1(t) = \sum_{m=0}^{n} a_m h\,(t - m\tau) \quad . \tag{2}$$

It has been shown[4] for a symmetrical $h(t)$, that if the input signal is fed into the other end of the tapped delay line through an

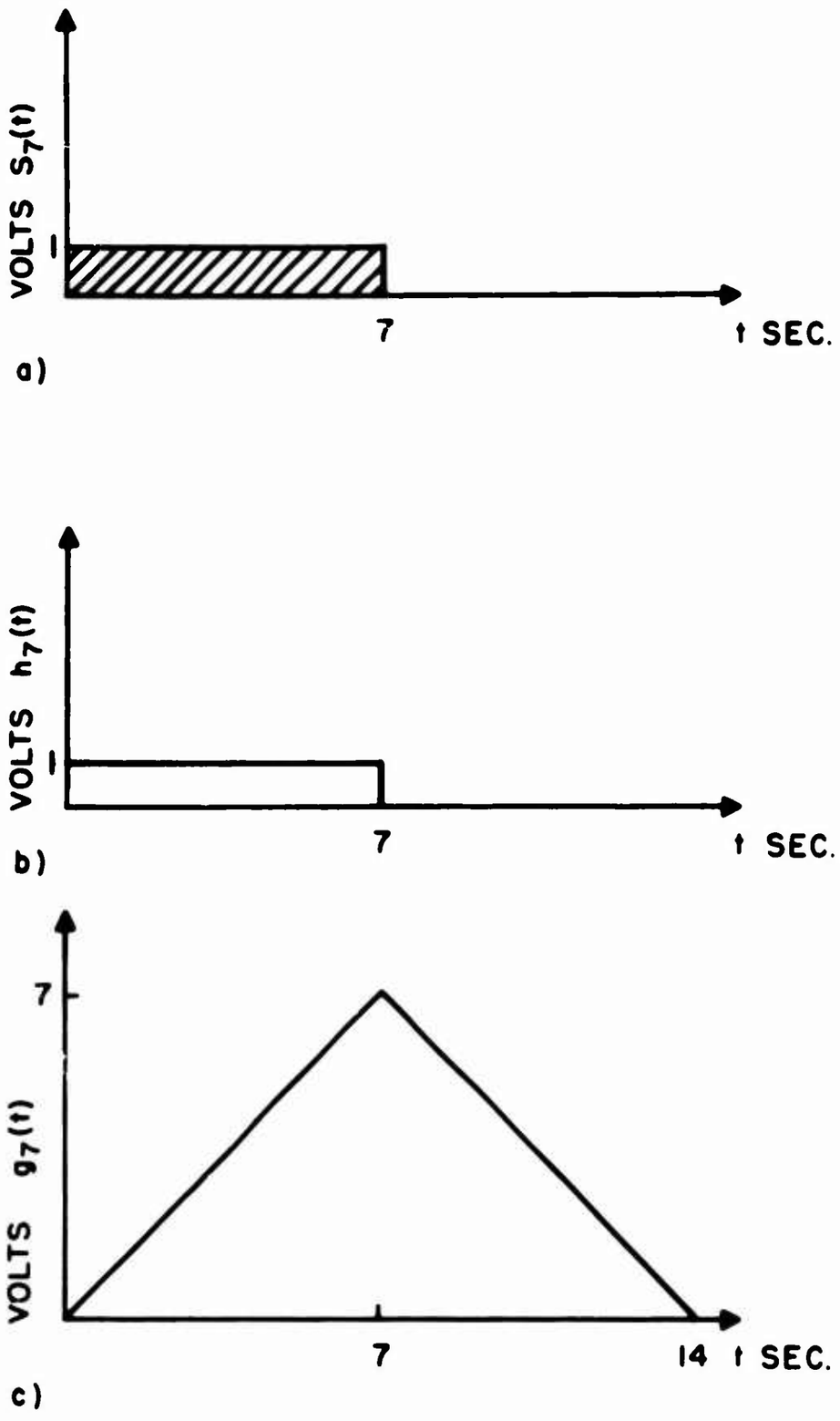

FIGURE 2 Effect of Increasing Signal Energy.
a) Input Signal. b) Impulse Response, c) Output Signal.

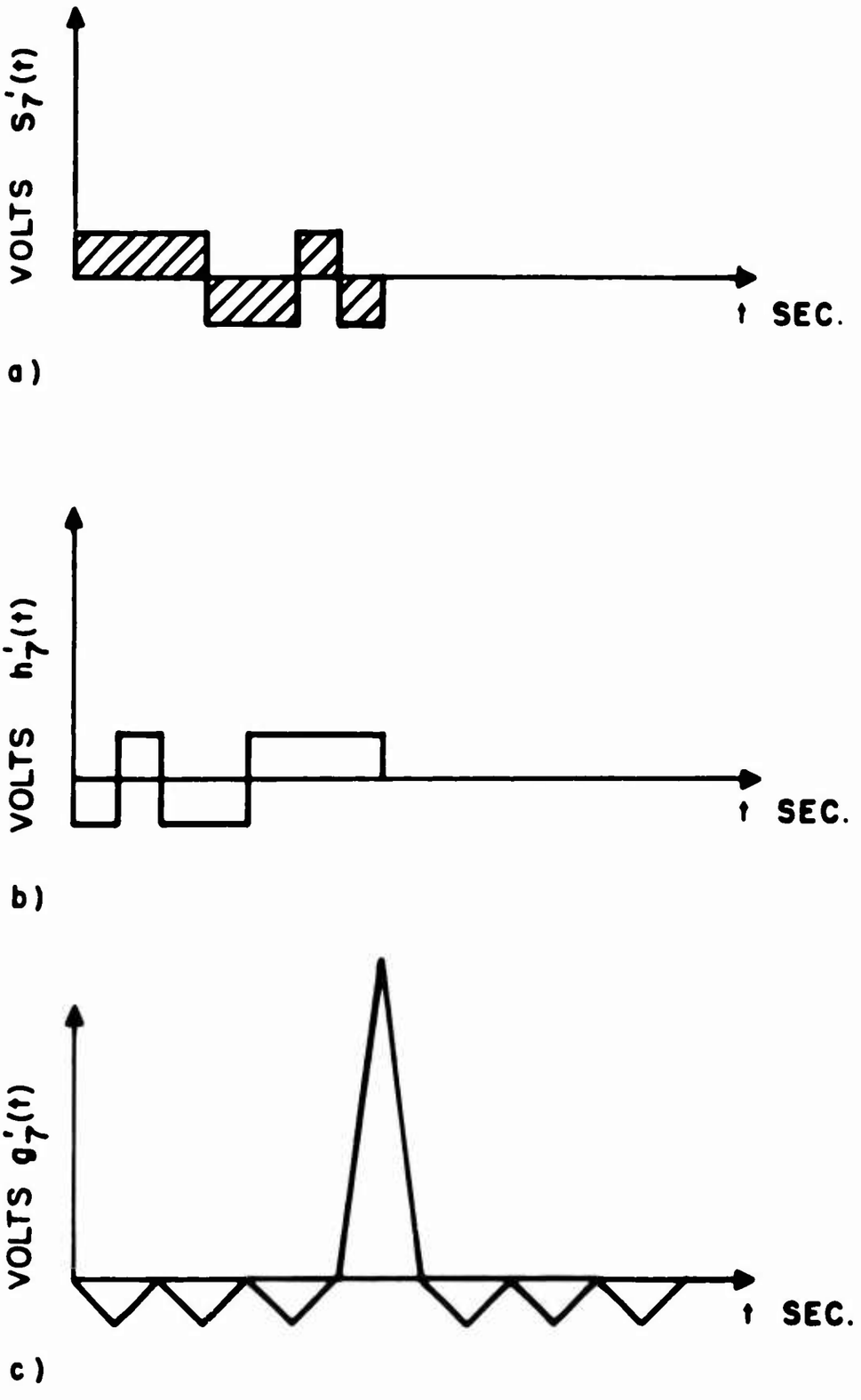

FIGURE 3. Effect of Coding the Signal, a) Coded Input Signal, b) Impulse Response, c) Output Signal.

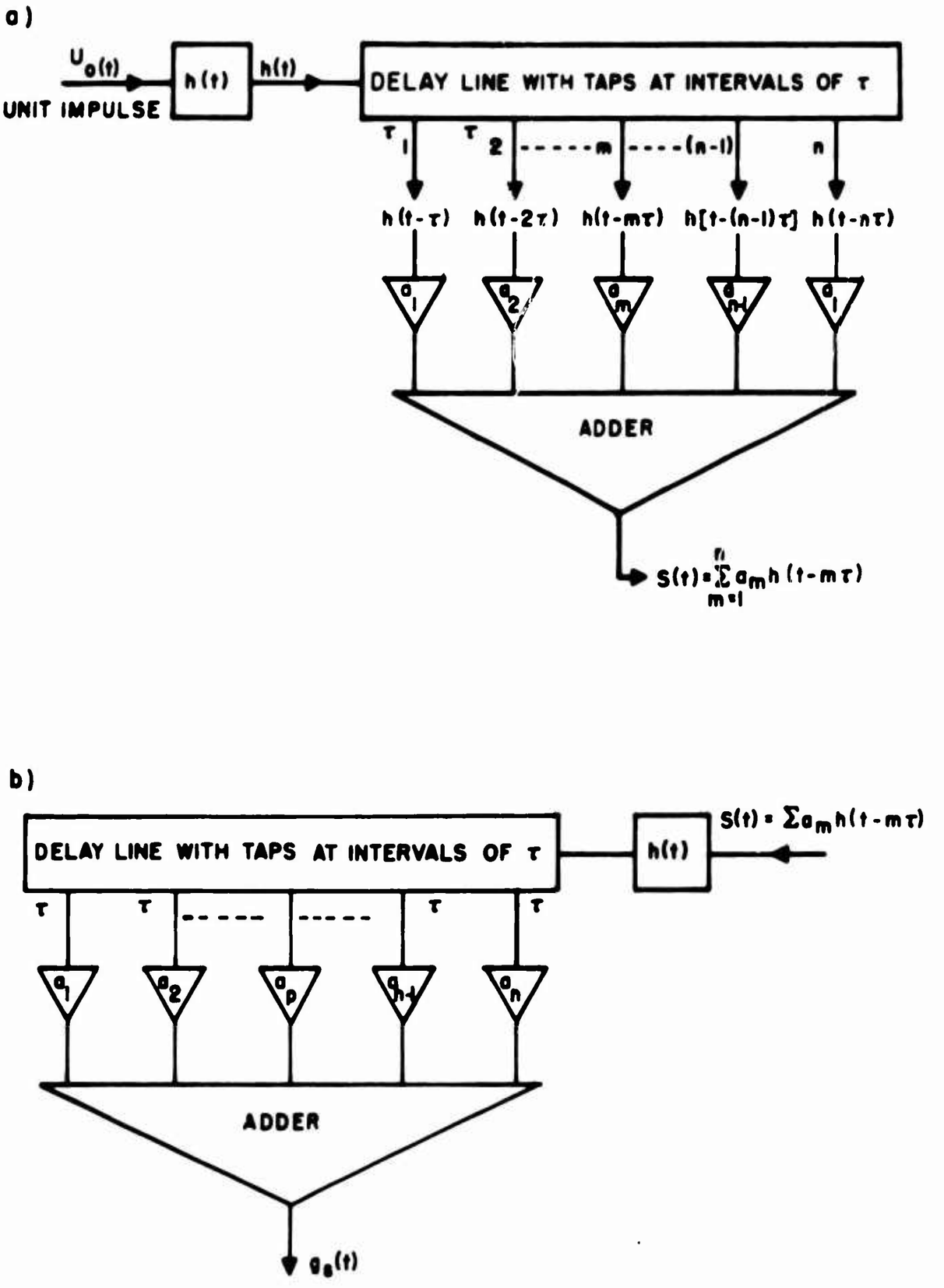

FIGURE 4. a) Idealized Coded-Pulse Generator, b) Matched Filter for Signal Generated by Coded-Pulse Generator of a).

identical prefilter, the same network used to generate the coded pulse may be used as a matched filter.

The possibility of lengthening and coding a pulse-like signal to improve the signal-to-noise ratio leads one to believe that there is no limit to the improvement in peak-signal-to-rms-noise ratio which may be obtained. Theoretically, the improvement is proportional to the square root of n, where n is the ratio of duration of the coded pulse to that of the original pulse. In practice, there are several factors which limit the improvement which may be obtained. In order to determine the influence of these physical limitations on the performance of coded-pulse generators and matched filters, a laboratory model of a seven-stage, wide-band signal generator and matched filter was constructed and evaluated.

II. THEORETICAL DISCUSSION

A. CHOICE OF NETWORK STRUCTURE

One approach to the design of signal generators and matched filters is to use a tapped-delay line and a summing device, as shown in Figure 4a. The output of the signal generator is the weighted sum of delayed replicas of $h_1(t)$ given by

$$s_1(t) = \sum_{m=0}^{n} a_m h_1(t - m\tau) \quad ,$$

where $h_1(t)$ is the prefilter impulse response.

A filter which is matched to this coded-pulse generator may be constructed in the same manner using a tapped-delay line and summing network to give an output:

$$s_2(t) = \sum_{m=0}^{n} b_m h_2(t - m\tau) \quad .$$

There is a useful relation between the weights of the matched filter and the weights of the signal generator. If the impulse response of the prefilter used in the matched filter $h_2(t)$ is related to that of the prefilter used in the signal generator by

$$h_2(t) = h_1(-t + T) \quad ,$$

and the relation between the weights is given by

$$b_m = a_{n-m} \quad ,$$

the impulse response of the matched filter will be

$$s_2(t) = \sum_{m=0}^{n} a_{n-m}\, h_1(-t + T + m\tau) \quad , \tag{3}$$

which satisfies the matched filter condition that $s_2(t) = s_1(-t + T_0)$ where the delay $T_0 = m\tau + T$.

These relations show how the same delay line, weights, and summing network used to generate a coded pulse may also be used as a filter matched to this coded pulse. Since $h_2(t) = h_1(-t + T)$, the prefilter impulse response should be symmetrical. The expression relating the weights ($b_m = a_{n-m}$) leads to the arrangement of Figure 4b, where the coded pulse is fed into the other end of the tapped-delay line.

The link structure[4, 5] offers an ingenious method of combining the operations of delay and summation (Figure 5). The geometry of the link structure allows wide-band operation by minimizing the effect of unavoidable stray capacitance. The stray capacitance is considered as part of the network in the synthesis procedure.

In order to simplify the explanation of the link structure, several assumptions of symmetry are made. These simplifying assumptions are by no means necessary. In fact, a much improved network resulted when one of these assumptions was relaxed, as will be reported later in this paper.

One of the assumptions made to simplify explanation is as follows: Each of the three-port networks represented as blocks in Figure 5

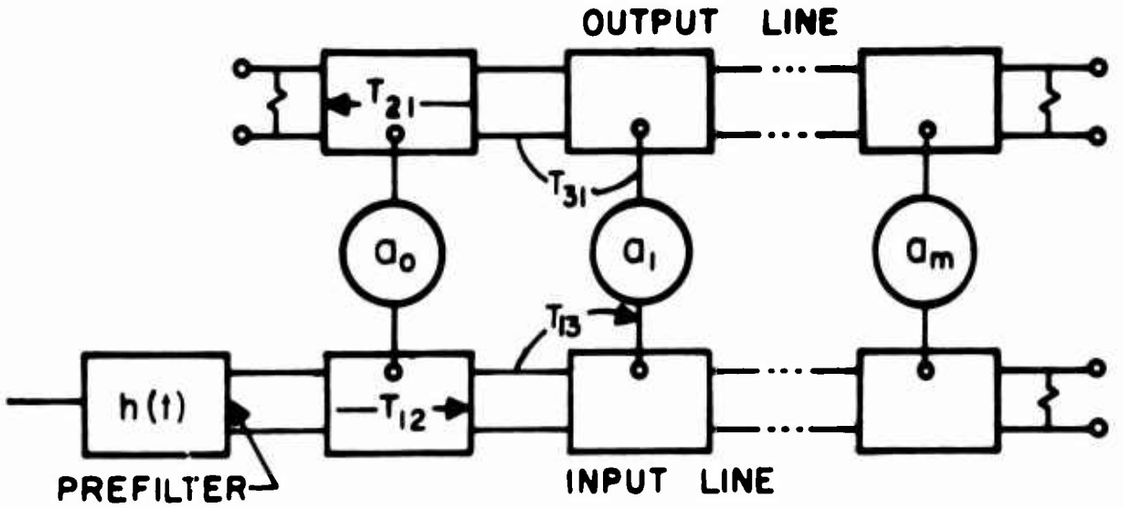

FIGURE 5 Link Structure.

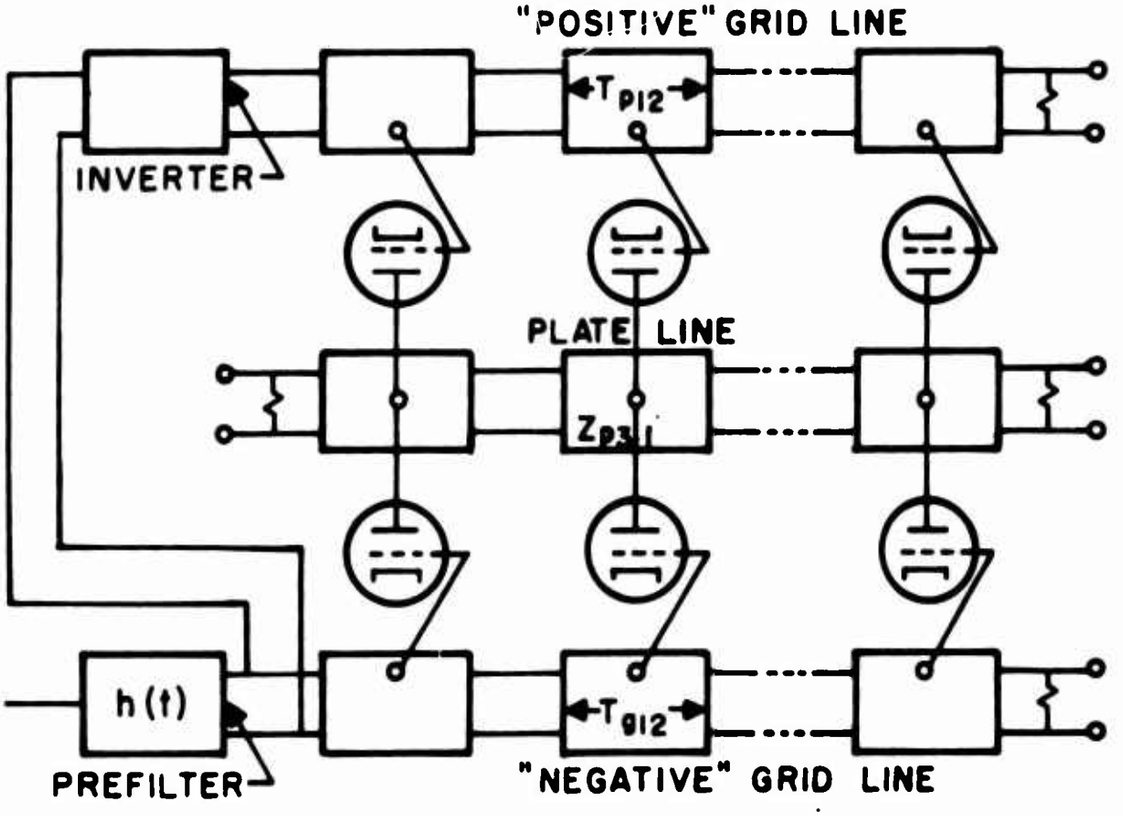

FIGURE 6 Schüssler's Structure.

is assumed to be symmetrical with identical voltage transfer ratios: $T_{12} = T_{21}$ and $T_{13} = T_{23} = T_{31} = T_{13}$.

For the link structure to behave as the tapped delay-line structure described, the m^{th} signal path should consist of a weight a_m and of a delay of mT. The actual transfer function of the m^{th} path in Figure 5 is given by

$$(T_{12})^m \quad T_{13} \quad a_m \quad T_{31} \quad (T_{21})^m \quad . \tag{4}$$

If T_{13} had no effect on the signal, $T_{13} = T_{31} = 1$, and if T_{12} represented an ideal delay of $T/2$, $(T_{12} = T_{21} = e^{-sT/2})$, then the effect of the m^{th} signal path on the output of the prefilter $h(t)$ would be given by

$$\left(e^{-s\frac{T}{2}}\right)^m \quad 1 \quad a_m \quad 1 \quad \left(e^{-s\frac{T}{2}}\right)^m = a_m \, e^{-smT} \quad ; \tag{5}$$

and the link structure would have the same behavior as the tapped-delay line and summing network, i.e.

$$s(t) = \sum_{m=0}^{n} a_m \, h(t - mT) \quad .$$

In this design of a wide-band link structure, vacuum tubes were used to implement the weights or coefficients a_m. In accordance with the use of vacuum tubes, a new terminology is introduced for the description of the various elements of the link structure. The input line of Figure 5 is referred to as the "grid line," and the output line

is referred to as the "plate line." The individual weights or gains are determined by the transconductance of the tube and the impedance level of the plate line, $a_m T_{31} = g_m Z_{31/2}$.

In general, as suggested in Figure 4, some weights will be positive and some will be negative. The negative weights can be easily realized by a single wide-band vacuum-tube circuit. However, the implementation of a positive weight leads to a cascade of two-vacuum tubes and the familiar problems in wide-band cascade amplifiers (principally the gain-bandwidth limitation). In order to avoid the use of positive weights and the attendant bandwidth limitations, Schüssler suggested the use of two grid lines, as shown in Figure 6.

In Figure 6, the grid line preceded by an inverter leads to a positive output signal and is therefore referred to as the positive grid line. The line connected directly to the prefilter leads to a negative output and is referred to as the negative grid line. A new notation is used to describe the transfer functions of the various blocks in Figure 6: T_{g12} represents the voltage transfer ratio of the grid-line sections; T_{p12}, the voltage transfer ratio of the plate-line sections; Z_{p31}, the transfer impedance ratio for the plate line. It is assumed that all grid-line sections are identical and symmetrical ($T_{g12} = T_{g21}$). It is also assumed that all plate-line sections are identical and symmetrical, although not necessarily the same as the grid-line sections.

In order to determine how the individual elements of Figure 6 should be designed, an expression for the transfer function in terms of the individual elements is compared with the desired over-all

transfer function. The k^{th} signal path has a transfer function given by

$$H_0(s) \left(T_{g12}(s)\right)^k \; T_{g13}(s) \; -g_m \; Z_{p31}(s) \left(T_{p12}(s)\right)^k \; .$$

The desired transfer function for the k^{th} signal path is

$$H(s) \left(T(s)\right)^k \; a_k \quad , \tag{6}$$

where $\left(T(s)\right)^k = \left(e^{-sT}\right)^k$ represents a delay of kT, $H(s)$ determines the shape of the individual pulse, and a_k represents the weight or coefficient associated with the k^{th} path.

A comparison of expressions (3) and (4) shows how the individual elements could be designed to give the desired over-all transfer function. The delay operation may be associated with the grid- and plate-line sections:

$$T(s) = T_{g12}(s) \; T_{p12}(s) = e^{-sT} \quad . \tag{7}$$

This expression implies that the grid and plate sections should have the characteristics of all-pass delay-line sections. In order to better compare the elements determining the weight or gain, the term $-g_m Z_{p31}(s)$ may be considered as $-g_m (R/2) T_{p31}(s)$, where R represents the resistance level of the plate line, $(R/2)T_{p31}(s)$ represents the transfer impedance $Z_{p31}(s)$, and $-g_m(R/2)$ becomes associated with the weight a_k in Expression (4). Thus, the gain through the k^{th} path is determined by the transconductance of the k^{th} tube and the impedance level of the plate line. The remaining terms determine

the shape of the pulse,

$$H_0(s)\ T_{g13}(s)\ T_{p31}(s) = H(s) \quad . \tag{8}$$

Expression (8) shows that the individual pulse shape is determined not only by the prefilter, but also by the delay line (plate and grid lines). As mentioned in the introduction, the design of the delay line is dependent upon the shape of the prefilter output, specifically the width or duration of the pulse. Since the effect of the delay line on the pulse shape cannot be determined by any simple analytic means, an iterative procedure using both analog and digital computers was used to determine a good design for the prefilter.

B. DESIGN OF THE PREFILTER

The prefilter has the major influence on the shape of the individual pulse. Expression (8) shows that the delay line also affects the shape of the pulse. For the delay lines considered in this case, the poles of T_{g13} and T_{p31} were spaced away from the poles of the prefilter (Figure 7), indicating that the effect of the delay line was slight and that perhaps the poles of the prefilter could be changed slightly to compensate for the distortion caused by T_{g13} and T_{p31}. Schüssler[7] has discussed the problem of the choice of the prefilter and has shown that if $h_1(t)$, the impulse response of the prefilter, is symmetrical (either an even or an odd function of time), the same prefilter may be used for both the signal generator and the matched

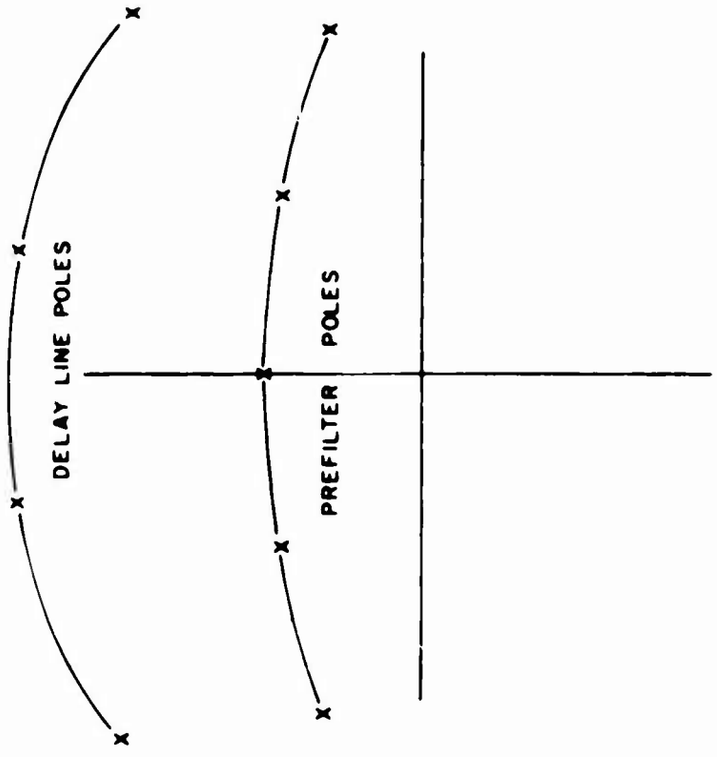

FIGURE 7. Relative Locations of Poles for Prefilter and Delay Line.

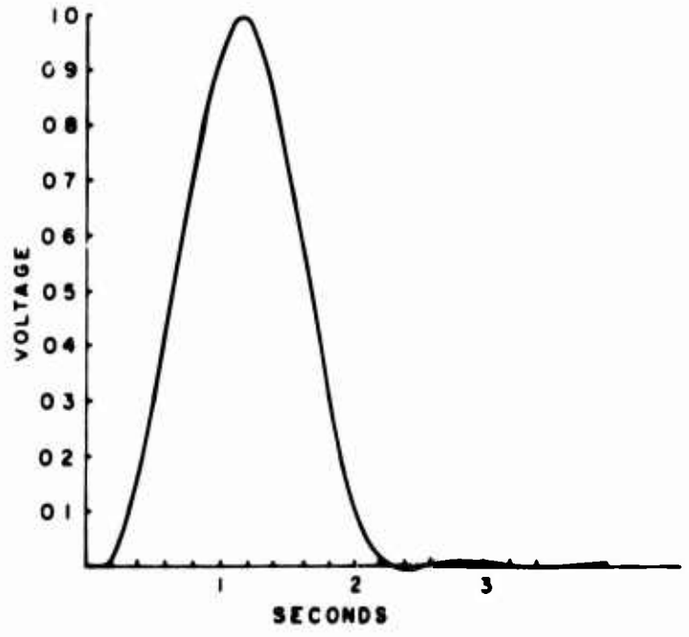

FIGURE 8. Impulse Response of Schüssler's Filter.

filter: $h_2(t) \pm h_1(t)$. The prefilter used in this design is a slightly modified version of a filter presented in another of Schüssler's papers. It will be referred to as Schüssler's filter for the remainder of this paper. This filter has 5 poles, 2 zeros, 1 percent overshoot for its impulse response, and a frequency stop-band transmission of 1 per cent or -40 db. It was chosen as a good compromise between simplicity demanded by wide-band operation and the complexity required to closely approximate the rectangular pulse. As shown in Figure 8, the impulse response of this filter comes close to being an even function of time.

Once the prefilter was chosen, the next step was to slightly modify the elements to compensate for the effect of the delay line on pulse shape. In the iterative procedure used, the prefilter and the delay line were set up on an analog computer using one potentiometer for each element of the prefilter (see Figure 9). First, the computer settings were determined assuming no interaction between the delay line and the prefilter. As expected, the resulting pulse was widened by the effect of the delay line. Next, time-scaling the parameters of the delay line, the width of the pulse at half-amplitude and the delay were adjusted to be the same. The final step in this procedure was to slightly change the setting of the potentiometer representing the final inductor in the prefilter, to compensate for the distortion of pulse shape (mostly increased overshoot) which resulted from the effect of the delay line. The set of potentiometer readings was then used to calculate by digital computer the new transfer function for the

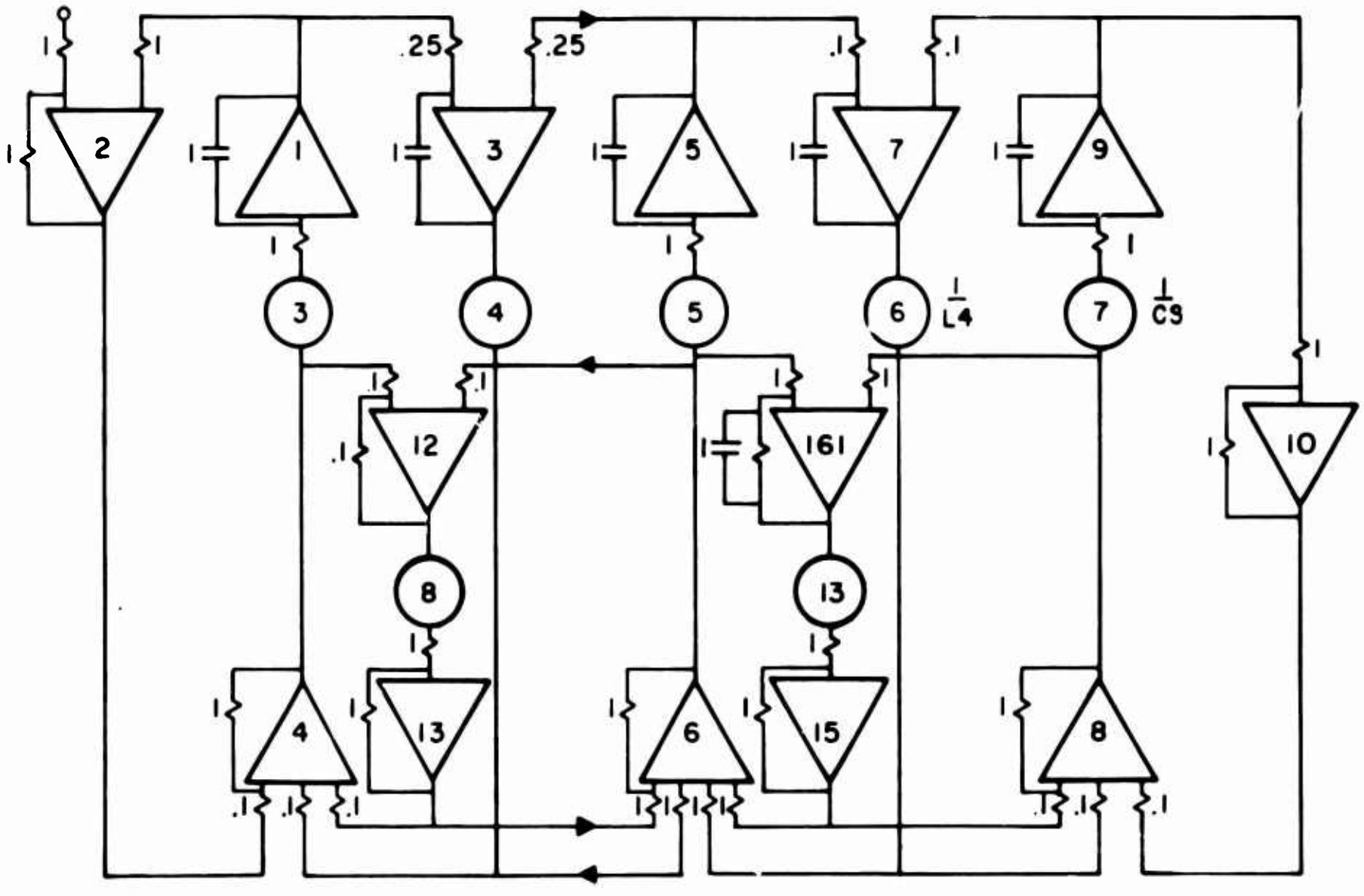

FIGURE 9. Analog-Computer Study of Prefilter.

prefilter. The results of this computer method are shown in Figures 10 and 11. The normalized transfer function of the prefilter before modification was

$$\frac{E_2}{E_1} = \frac{0.88\,s^2 + 1}{36.2\,s^5 + 51.9\,s^4 + 56.0\,s^3 + 33.5\,s^2 + 12.3\,s + 2} \quad . \tag{9}$$

After changing potentiometer No. 6 from 0.757 to 0.900, the resulting modified transfer function was

$$\frac{E_2}{E_1} = \frac{0.88\,s^2 + 1}{36.2\,s^5 + 48.9\,s^4 + 56.0\,s^3 + 33.5\,s^2 + 12.3\,s + 2} \quad . \tag{10}$$

The frequency responses both of the original prefilter and of the modified prefilter are shown in Figure 12.

C. DESIGN OF GRID AND PLATE LINES

The transfer functions of the sections of the grid and plate lines should approximate e^{-sT}. Each section of the line should delay the individual pulse without distortion. Since there is no convenient method of designing delay-line sections for a specified behavior in the time domain, the following discussion considers the frequency response of the delay line.

The delay of a network is proportional to the slope of the phase angle versus frequency plot, or the phase slope. The requirement that the network delay a wide-band signal without distortion leads to

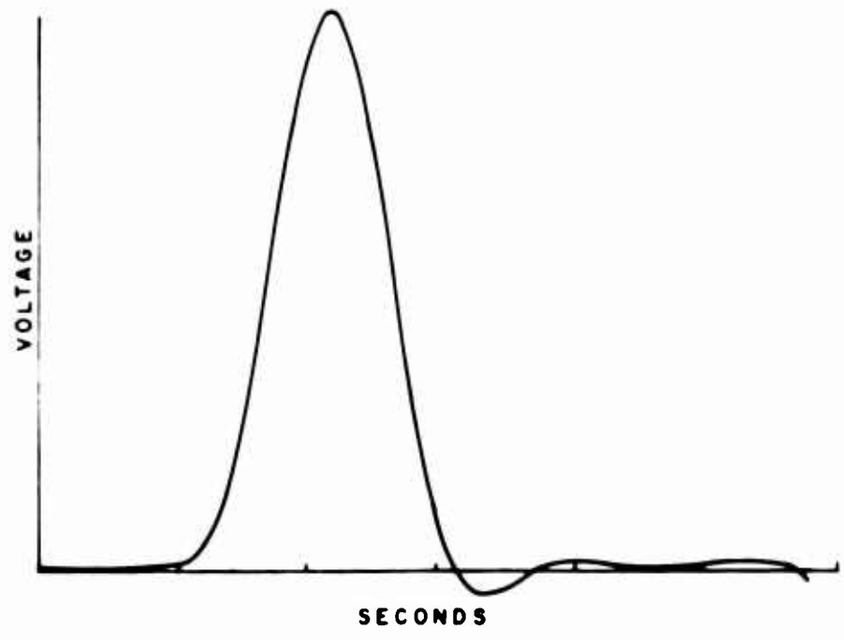

FIGURE 10. Effect of Delay Line on Prefilter Output.

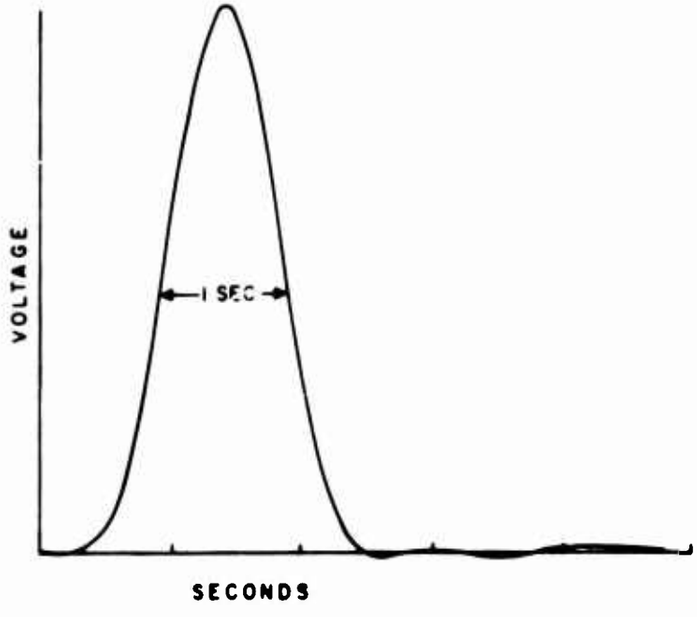

FIGURE 11. Effect of Modification to Reduce Overshoot.

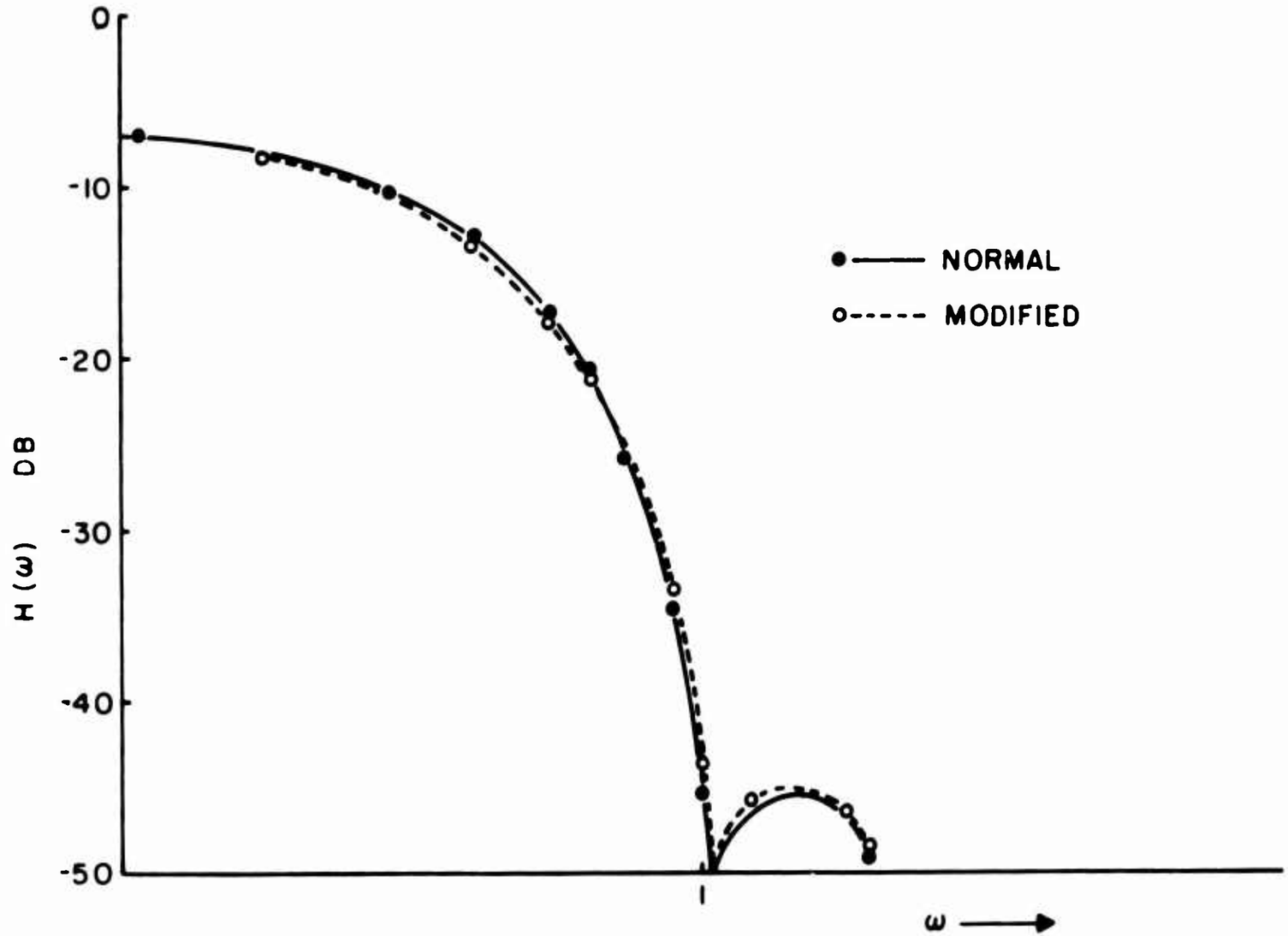

FIGURE 12 Prefilter Frequency Response.

the requirement that the network provide the same delay for a wide range of frequencies. This, in turn, means that the phase slope should be constant, which requirement leads to the choice of a "linear-phase" network. Since, for this particular application, the low-frequency delay appeared to be most important, a network which provides the minimum error in delay at low frequencies was chosen. The delay-line section design was based on the Bessel polynomials. Figure 13 shows how the error in delay is zero at the origin and gradually increases with frequency for a Bessel delay line.

The combination of one section of grid line and one section of plate line should provide a total delay of T. For convenience, the plate and grid lines were at first designed to be identical, each with a delay of T/2. This is the procedure when the link structure is used as a wide-band amplifier. It was decided to use constant-resistance networks for the individual sections of the delay line so that the transfer function of the entire line would simply be the product of the individual transfer functions. The input impedance of a constant-resistance network when terminated in its characteristic resistance is simply the characteristic resistance. Therefore, this terminated constant-resistance network may itself be used to terminate a similar network.

The use of a balanced lattice network[8] provides a convenient synthesis procedure for constant-resistance all-pass networks. Figure 14 shows a balanced lattice network terminated in one ohm. If $Z_a Z_b = 1$, the input impedance of the lattice will be one ohm. This

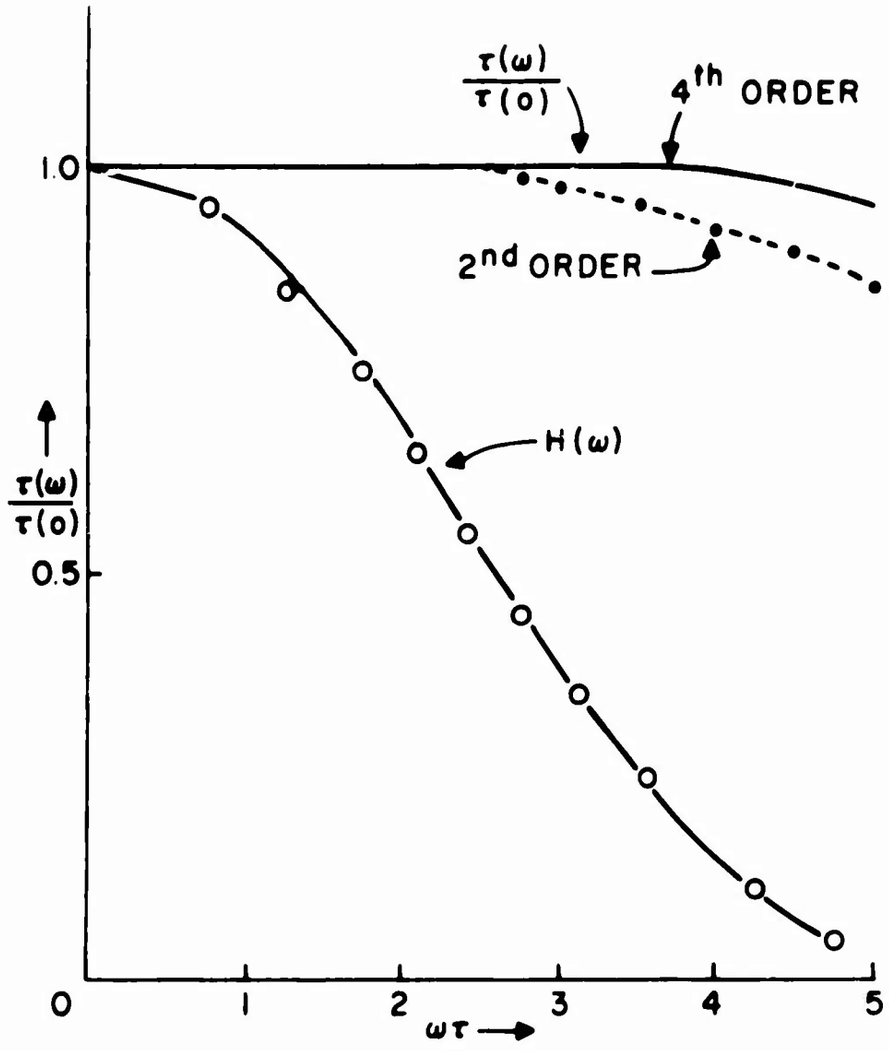

FIGURE 13. Comparison of Second-Order and Fourth-Order Bessel Polynomial Approximations to Flat Delay.

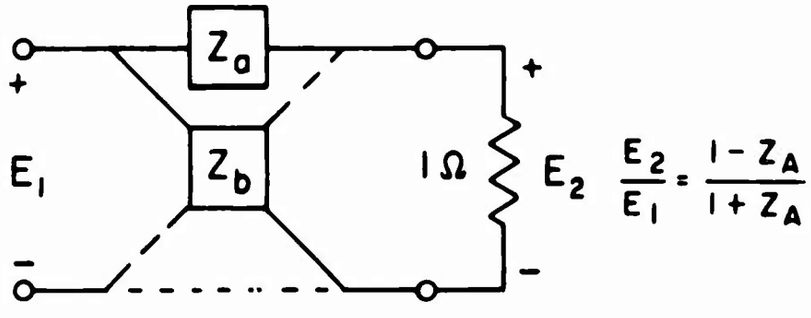

FIGURE 14. Balanced Lattice Network.

constant-resistance lattice then has a transfer function given by

$$T_{12}(s) \quad \frac{E_2(s)}{E_1(s)} \quad \frac{1 - Z_a(s)}{1 + Z_a(s)} \quad . \tag{11}$$

The individual impedances Z_a and Z_b may be determined from the transfer function, as shown:

$$Z_a(s) \quad \frac{1 - T_{12}(s)}{1 + T_{12}(s)} \quad , \qquad Z_b(s) \quad \frac{1 + T_{12}(s)}{1 - T_{12}(s)} \quad . \tag{12}$$

For a second-order all-pass network, the desired transfer function is

$$T_{12}(s) = \frac{E_2(s)}{E_1(s)} = \frac{P(-s)}{P(s)} \quad \frac{s^2 - a_1 s + a_0}{s^2 + a_1 s + a_0} \quad . \tag{13}$$

Thus,

$$Z_a(s) \quad \frac{s^2 + a_1 s + a_0 - s^2 + a_1 s - a_0}{s^2 + a_1 s + a_0 + s^2 - a_1 s + a_0} \quad \frac{a_1 s}{s^2 + a_0} \quad ,$$

and

$$Z_b(s) \quad \frac{1}{Z_a(s)} \quad \frac{a_1}{s} + \frac{a_1}{a_0} s \tag{14}$$

These individual impedances may be realized by lossless networks consisting of one inductor and one capacitor, as shown in Figure 15:

$$Z_a(s) \quad \frac{1}{sC + \frac{1}{sL}} = \frac{sL}{s^2 LC + 1} = \frac{s\left(\frac{1}{C}\right)}{s^2 + \left(\frac{1}{LC}\right)} \quad .$$

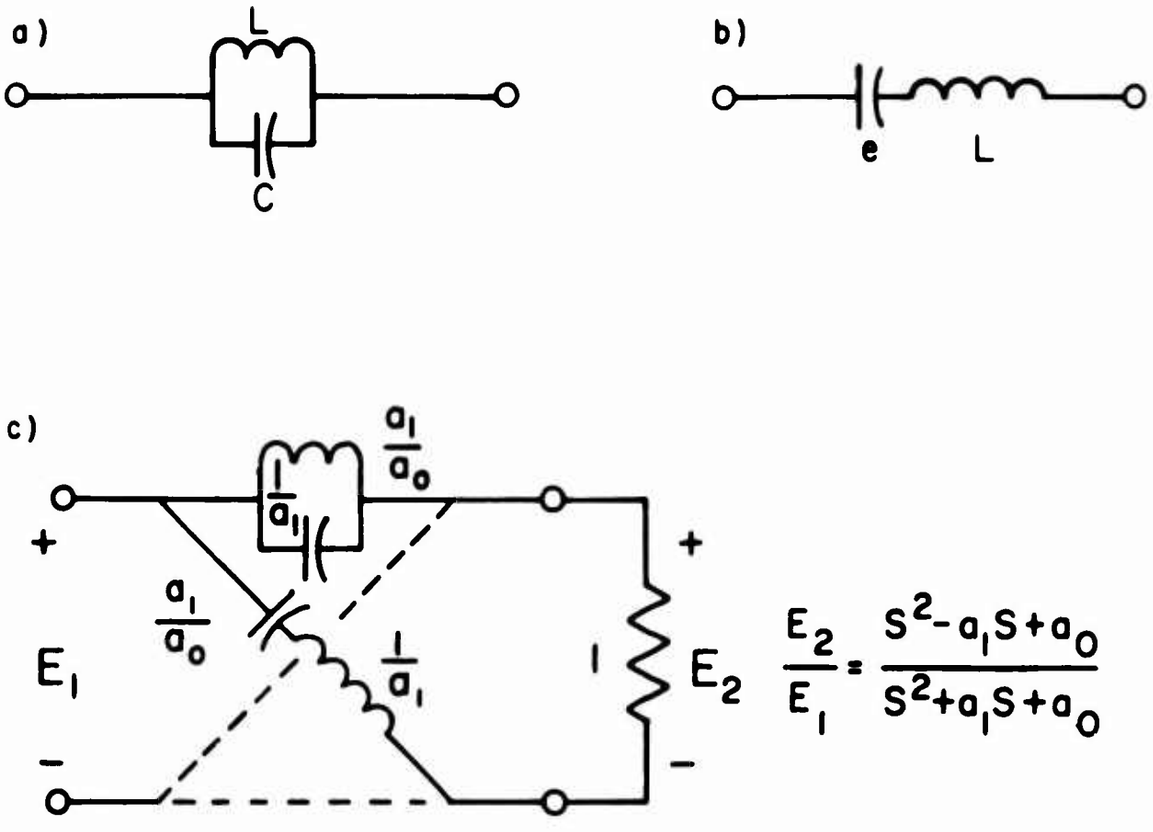

FIGURE 15. Balanced LC Lattice.

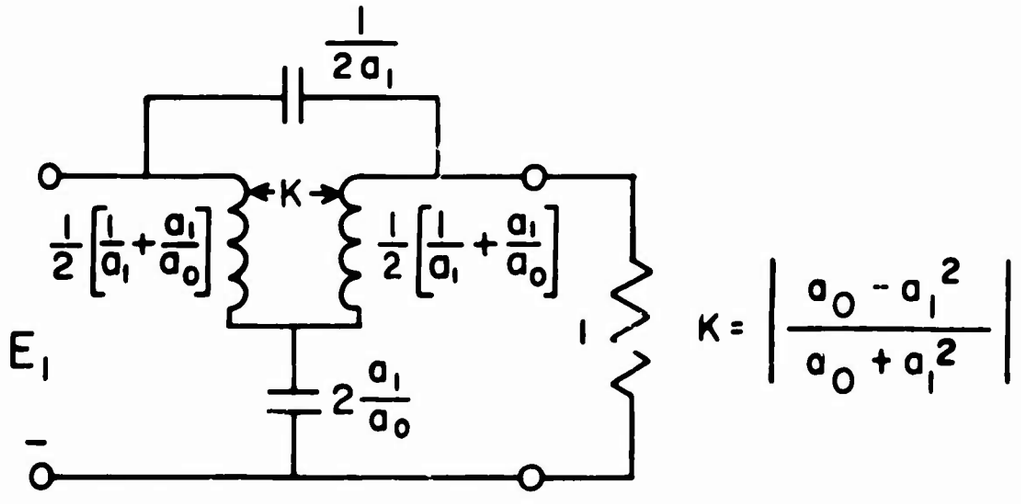

FIGURE 16. Unbalanced Lattice

$$Z_b(s) = \frac{1}{sC} + sL \quad . \tag{15}$$

The balanced LC lattice incorporating this Z_a and Z_b is shown in Figure 15. The lattice in this form presents several practical difficulties, such as the lack of a common ground terminal for input and output. A more practical unbalanced form of the lattice is shown in Figure 16. This unbalanced lattice also presents a major problem in construction, especially at high frequencies, in that the coupled coils are quite difficult to construct. However, the following discussion shows that coupled coils are necessary when the transfer function designed from Bessel polynomials is required to have the flat delay characteristic of Figure 13.

The coupled coils are shown in Figure 17; the open-circuit impedance parameters for this network are

$$z_{11} = z_{22} = sL \quad , \quad z_{12} = skL \quad .$$

The T network in Figure 18 has the same open-circuit impedance parameters,

$$z_{11} = z_{22} = (1-k)sL + ksL = sL \quad ,$$

$$z_{12} = skL \quad ,$$

and is therefore equivalent to the pair of coupled coils. This T network of three inductors with no coupling may be realized if k is non-negative. However, the coupling coefficient cannot be non-negative because of the following relations between the coefficients of the

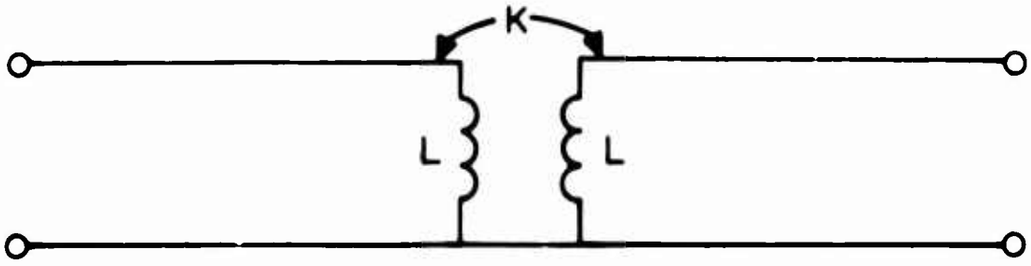

FIGURE 17. Coupled Coils.

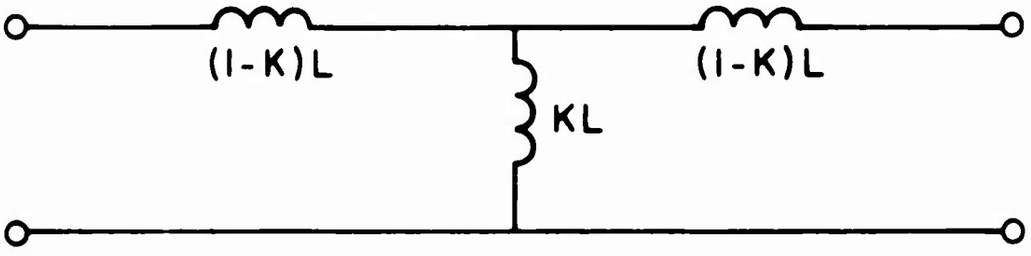

FIGURE 18. Equivalent Circuit for Coupled Coils.

second-order Bessel polynomials.

For

$$\Gamma(s) \quad \frac{P(-s)}{P(s)} \quad \frac{s^2 - a_1 s + a_0}{s^2 + a_1 s + a_0} \quad ,$$

the phase angle is given by the expression,

$$\phi(\omega) \quad -2\tan^{-1} \frac{a_1 \omega}{a_0 - \omega^2} \quad -2\tan^{-1} \frac{m}{n} \quad , \tag{16}$$

the phase slope is given by the expression,

$$\phi'(\omega) \quad \frac{-2}{1 + \frac{m^2}{n^2}} \left[\frac{m'n - n'm}{n^2} \right] \quad -2 \left[\frac{m'n - n'm}{m^2 + n^2} \right] \tag{17}$$

Where

$$m = a_1\omega \,, \qquad m' = a_1 \,,$$

$$n = a_0 - \omega^2 \,, \qquad n' = -2\omega \,,$$

the phase slope is given by

$$\phi'(\omega) = -2\,\frac{a_1a_0 - a_1\omega^2 + 2a_1\omega^2}{a_1^2\omega^2 + a_0^2 - 2a_0\omega^2 + \omega^4} \,. \tag{18}$$

At the origin, the delay is given by

$$\phi'_{(0)} = -2\,\frac{a_1a_0}{a_0^2} = -2\,\frac{a_1}{a_0} \,, \quad \text{or} \quad \tau(0) = \frac{2a_1}{a_0} \,. \tag{19}$$

For a constant delay, at least near $\omega = 0$, the phase slope should be of the form

$$\phi'(\omega) = \frac{-2a_1}{a_0}\left[F(\omega)\right] \,, \tag{20}$$

where $F(\omega)$ is approximately 1 for small ω. Since

$$F(\omega) \quad \frac{a_0^2 + a_0\omega^2}{a_0^2 + \left(a_1^2 - 2a_0\right)\omega^2 + \omega^4} \,,$$

the relation $a_0 \quad a_1^2 - 2a_0$ will make

$$F(\omega) = \frac{1}{1 + \dfrac{\omega^4}{a_0^2 + a_0\omega^2}} \sim 1 \tag{21}$$

for small ω.

The use of the Bessel polynomial approximation for maximally flat delay thus requires that $a_1^2 = 3a_0$. The coupling coefficient is

$$k = \left(\frac{a_0 - a_1^2}{a_0 + a_1^2} \right) = \frac{\frac{a_1^2}{3} - a_1^2}{\frac{a_1^2}{3} + a_1^2} ,$$

or

$$k = \frac{-\frac{2}{3}}{\frac{4}{3}} = \underline{\underline{-0.5}} . \qquad (22)$$

These relations show that the coupling coefficient must be negative, as long as $a_1^2 > a_0$ and, in fact, must be equal to minus one-half when the Bessel polynomial approximation to linear phase is used in connection with a second-order network. The requirement for a coupling coefficient of one-half causes difficulties, especially at high frequencies and for the plate line. As mentioned earlier, the gain for an individual signal path depends on the transconductance of the vacuum tube and the impedance level of the plate line. Thus, it is desirable to have a high plate-line impedance. However, high impedance implies large inductance and small capacitance values. Large, closely coupled coils lead to large values of stray capacitance. Therefore, it is desirable to consider a different plate line which does not require such close coupling of coils.

If the assumption of identical grid and plate sections is abandoned, a plate line with smaller coupling may be synthesized. One

drawback, however, of nonidentical grid and plate sections is that the structure may not be used as an ordinary wide-band amplifier.

The development of the nonidentical delay sections begins by realizing that the only requirement is that the combination represented by $T_{g12}T_{p21}$ be a good delay line; the individual sections represented by T_{g12} and T_{p21} need not be. Instead of considering the cascade as two second-order networks, the combination is considered as one fourth-order network in two parts, or sections. While neither section by itself is a good, all-pass delay line, the combination, based on a fourth-order Bessel polynomial, has much less error in delay than the cascade of two networks based on second-order polynomials (Figure 13). This improvement is obtained with no increase in network complexity. Both lines still consist of two coupled coils and two capacitors.

The over-all transfer function provided by the combination should be of the all-pass form,

$$\frac{s^4 - a_3 s^3 + a_2 s^2 - a_1 s + a_0}{s^4 + a_3 s^3 + a_2 s^2 + a_1 s + a_0} \quad , \tag{23}$$

with a pole-zero plot, as shown in Figure 19. The over-all transfer function T(s) may be written as the product of two second-order polynomials:

$$\frac{\left(s^2 - a_1^{(1)} s + a_0^{(1)}\right)}{\left(s^2 + a_1^{(1)} s + a_0^{(1)}\right)} \cdot \frac{\left(s^2 - a_1^{(2)} s + a_0^{(2)}\right)}{\left(s^2 + a_1^{(2)} s + a_0^{(2)}\right)} \quad . \tag{24}$$

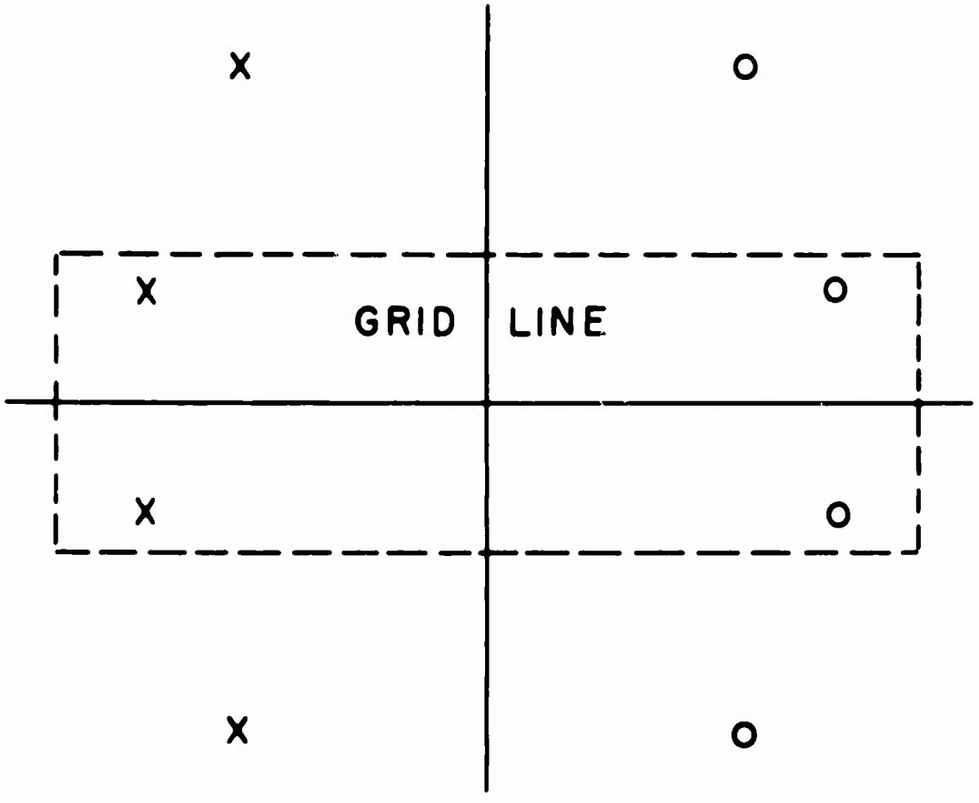

FIGURE 19. Fourth-Order Pole-Zero Plot for Bessel Polynomial.

The polynomial with superscript 1 is represented by the poles and zeros enclosed within the dashed lines in Figure 19, and the polynomial with superscript 2 is represented by the other two poles and the two zeros, which have their major influence at higher frequencies. As shown below, polynomial 2 requires a coupling coefficient less than one-half, and therefore may be used in the plate line at a higher impedance level than that permitted by the identical second-order grid and plate lines which were first considered. The polynomial 1, when used to synthesize the grid line, reduces the loading effect of

the grid line on the prefilter, as described in the section on design and construction. The coupling coefficients required when a fourth-order Bessel polynomial is used as a basis for the combined transfer function of two second-order networks may be derived from

$$T(s) = \left(\frac{s^2 - a_1^{(1)} s + a_0^{(1)}}{s^2 + a_1^{(1)} s + a_0^{(1)}} \right) \left(\frac{s^2 - a_1^{(2)} s + a_0^{(2)}}{s^2 + a_1^{(2)} s + a_0^{(2)}} \right) ,$$

which may be written as

$$T(s) = T_1(s)\, T_2(s) \quad ; \tag{25}$$

where $T_1(s)$ is represented by the poles and zeros nearest the origin in Figure 19.

For $T_1(s)$, the coefficients are related by $a_1^2 = 3.7a_0$, therefore:

$$k = \frac{a_0 - a_1^2}{a_0 + a_1^2} = \frac{a_0 - 3.7a_0}{a_0 + 3.7a_0} = \frac{2.7}{4.7} ,$$

$$k = -0.575 . \tag{26}$$

For $T(s)$, the coefficients are related by $a_1^2 = 1.7a_0$, therefore:

$$k = \frac{a_0 - 1.7a_0}{a_0 + 1.7a_0} = -\frac{0.7}{2.7} ,$$

$$k = -0.26 . \tag{27}$$

III. DESIGN AND CONSTRUCTION

This section begins with the design of the prefilter, grid and plate lines, and gain elements; then concludes with a description of the layout and construction of the entire matched filter.

The design of the networks must take into account the physical properties of the elements used in construction. The stray capacitance shunting inductors, the inductance of interconnecting leads, the shunt capacitance across load resistors, etc. – all must be considered. Impedance and frequency scaling must also be used to trade gain for distortion-free operation. The arrangement of components on the chassis must be carefully considered to prevent unwanted coupling of circuits; shielding may be necessary; power leads must be bypassed.

A. DESIGN OF PREFILTER

A fifth-order ladder filter, with an impulse response which is approximately an even function of time, was chosen for a prefilter. The filter, with element values normalized for a one-ohm impedance level and a cutoff radian frequency of one, was taken from a paper by Schüssler[9] and is shown in Figure 20a. The parameters were adjusted in several steps to give the values used to construct the prefilter used in the 50 Mc/s matched filter. The pulse width of the Schüssler filter with a cutoff frequency ω of one is $T = 2\pi M$, where T is measured between the 1-percent amplitude points, and where M,

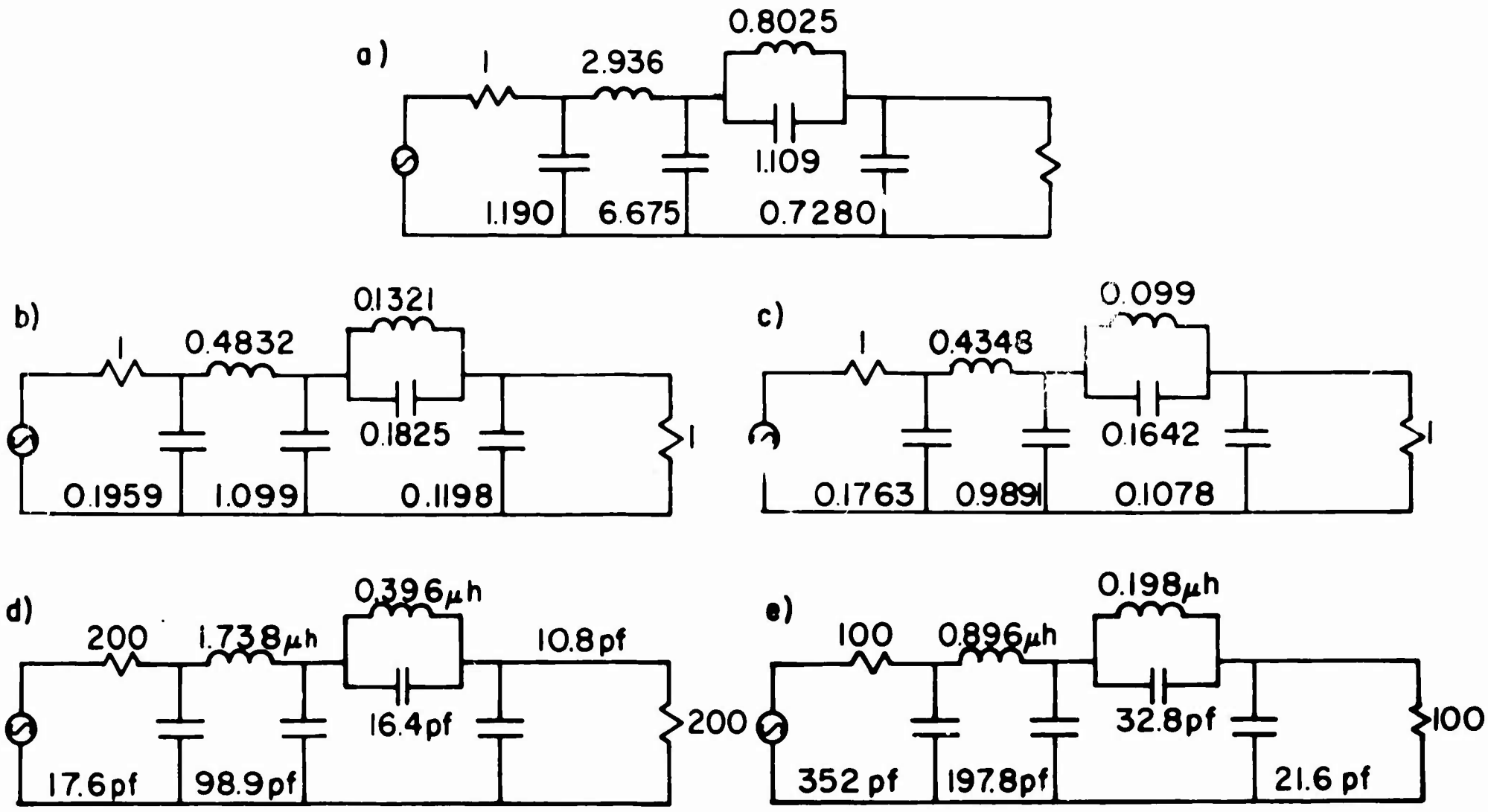

FIGURE 20. Development of Prefilter, a) Schüssler's Filter, b) through d) Scaled Versions, e) Prefilter Used.

a measure of time bandwidth product, equals $(\omega/2\pi)T$. Since $T/2$ is the delay per section of the grid and plate lines, the prefilter is normalized to give a 2-sec pulse width, thus requiring a 1-sec delay. The capacitors and inductors are multiplied by $1/\pi M$ to give the filter shown in Figure 20b.

The next parameter adjustment was the result of the analog-computer simulation described in section II. The final inductor was made smaller to compensate for the effect of $T_{g13}Z_{p31}$. To allow for widening of the pulse as it passed through the seven sections of delay line, the elements were scaled to give a 1.8-sec pulse width. The resulting filter is shown in Figure 20c.

The elements were again frequency-scaled to agree with the 20-ns delay of the actual matched-filter lines. The impedance level was also raised to 200 ohms, so that the filter could be terminated directly with the 200-ohm grid line. This network is shown in Figure 20d, where the capacitors have been multiplied by $2 \times 10^{-8}/200$ 100×10^{-12} and the inductors have been multiplied by 400×10^{-8} 4×10^{-6}. Measurement of the stray capacitance across the prefilter load showed that the specified 10.8 pf of Figure 20d was exceeded by stray capacitance. This forced the use of a lower impedance grid line and prefilter. The prefilter finally used had a 100-ohm impedance level with twice the allowable shunt capacitance across the load, as shown in Figure 20e.

B. DESIGN OF GRID AND PLATE LINES

As discussed in section II, it was decided to use a fourth-order Bessel polynomial as a basis for the design of the grid and plate sections. The normalized Bessel polynomial for a delay of one second is

$$\beta(s) = s^4 + 10s^3 + 45s^2 + 105s + 105 \quad . \tag{28}$$

As in section II, this polynomial is written as the product of two second-order polynomials:

$$\beta(s) = T_1(s)T_2(s) = (s^2 + 5.7924s + 9.1401)(s^2 + 4.2076s + 11.4872) \quad . \tag{29}$$

The lattice network used for the grid line was based on $T_1(s)$, while that used for the plate line was based on $T_2(s)$. The elements of the grid line were scaled to give a 100-ohm impedance level and an overall delay of 20 ns by multiplying the capacitors by 200×10^{-12} and multiplying the inductors by 2×10^{-6}. The coupling coefficient is unchanged by this scaling. The resulting 100-ohm grid-line section was used in the construction and is shown in Figure 21.

The elements of the plate line were scaled to give a 400-ohm impedance level. It was decided that 400 ohms is as high an impedance as is practical with the particular construction technique used. The stray capacitance of the coupled coils is about 2 pf, which is the same order as the shunt capacitance specified for a 400-ohm impedance level. In fact, even 400 ohms was too high for the plate section originally considered, which required a coupling coefficient of one-half, since the stray capacitance increased as the coils were brought

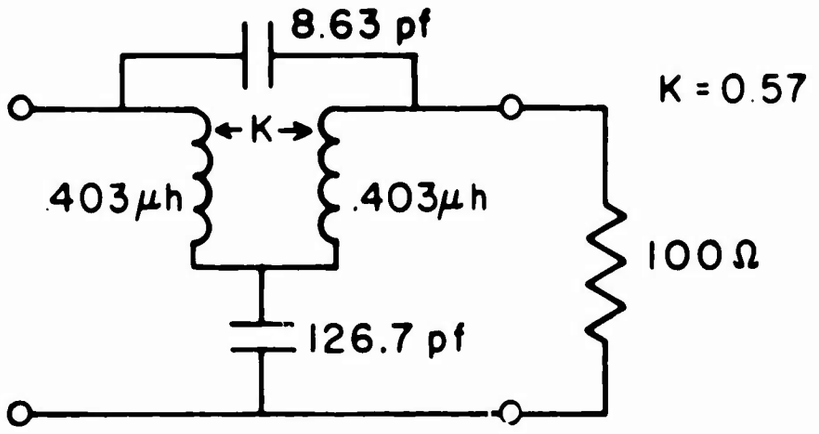

FIGURE 21 Grid-Line Section

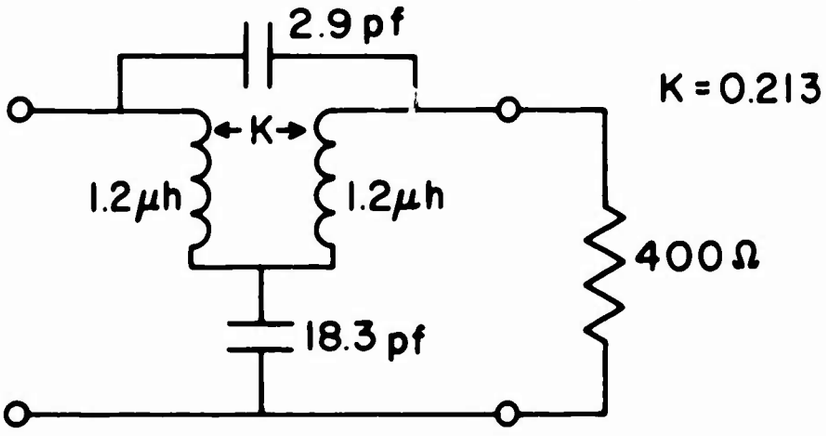

FIGURE 22. Plate-Line Section.

closer together to give more coupling. The resulting 400-ohm plate-line section used in construction is shown in Figure 22.

C. DESIGN OF GAIN ELEMENTS OR WEIGHTS

As mentioned earlier, vacuum tubes are used as the gain elements. The ideal active element would have an equivalent circuit which is a controlled current source with no stray capacitance as shown in Figure 23a. A vacuum tube with the equivalent circuit, shown in Figure 23b, approximates the ideal element. The two stray capacitances C_{in} and C_{out} may be taken into account as part of the grid and plate sections (Figure 24). The grid to plate capacitance C_{gp}, however, cannot be taken into account and should therefore be as small as possible. The best tube should have reasonably small values for C_{in} and C_{out}, but should have a very small C_{gp}; therefore, a pentode is suggested for this application. Since the gain coefficient a_k depends on g_m ($a_k = g_m R$), a high-g_m pentode is desirable. The 6DK6 tube was selected because of its high g_m combined with low interelectrode capacitance. The parameters of the 6DK6 tube are as follows:

$$\begin{aligned} E_b &= 125\,v, & C_{in} &= 6.3\,pf, \\ E_{g2} &= 125\,v, & C_{out} &= 1.9\,pf, \\ I_b &= 12\,ma, & C_{gp} &= 0.025\,pf, \\ R_k &= 50\,ohms, & a_m &\simeq 10,000\,\mu mho. \end{aligned} \tag{30}$$

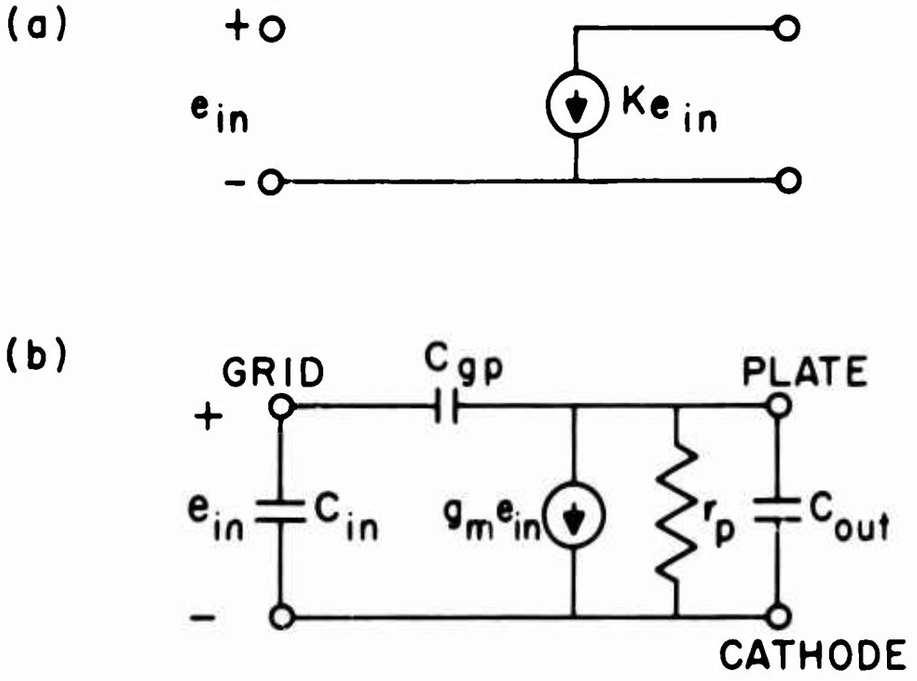

FIGURE 23. Equivalent Circuits for (a) Ideal Element, (b) Vacuum Tubes.

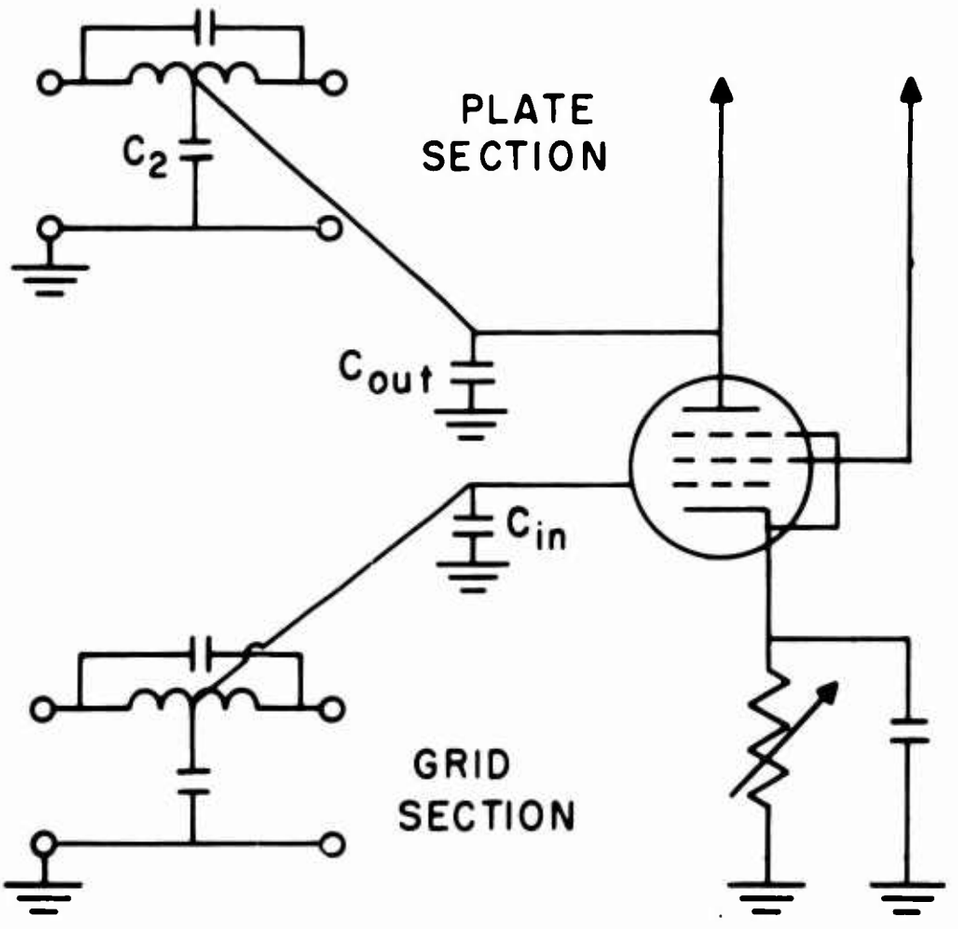

FIGURE 24. Amplifier with Associated Grid and Plate Networks.

In order to adjust the gain of the amplifier, a variable resistor was provided to vary the operating point of the tube (Figure 24).

D. CONSTRUCTION

The aim in developing the layout was to separate the biasing circuitry from the signal-carrying circuitry. The tubes, bias resistors, filament leads, and power leads are all underneath the chassis. In order to prevent coupling between stages, the bias leads are all bypassed to the chassis with short leads on the bypass capacitors. Above the chassis, the two grid lines run along the edges while the plate line runs down the center. The axes of the grid and plate coils are perpendicular to each other in order to minimize magnetic coupling. The leads connecting the sections of grid and plate line together were made as short as possible to minimize the lead inductance. At the same time, care was taken to keep the coils as far apart as possible to minimize magnetic coupling. The coils were also spaced away from the chassis to minimize stray capacitance to ground. Two tube sockets were provided for each section in order to provide a convenient means of changing the coefficients a_k.

The signal appearing at the k^{th} section of plate line is given by

$$E_p = g_{mk}^{+} R \quad e_k^{+} + g_{mk}^{-} R \quad e_k^{-} \quad . \tag{31}$$

The symbol g_{mk}^{+} represents the transconductance of the tube associated with the positive grid line, while g_{mk}^{-} represents the transconductance

of the other tube connecting the negative grid line to the plate line. Similarly, e_k^+ and e_k^- represent the signals at the k^{th} taps on the positive and negative grid lines, respectively. Normally e_k^- is simply the negative of e_k^+, and the expression for E_p may be simplified to read

$$E_p = e_k^+ \left[g_{mk}^+ - g_{mk}^-\right] R \quad . \tag{32}$$

In this manner the coefficient a_k may be set to any value between $+g_{mk}^+R$ and $-g_{mk}^-R$. This method of obtaining variable coefficients appears easier to implement at high frequencies than that proposed by Ganapathy.[10]

With the code chosen, only one tube per section was used. The other tube socket was provided with a dummy plug to simulate the tube interelectrode capacitances so that it was not necessary to readjust the network parameters when the code was changed

Standard-composition resistors, disk ceramic and feedthrough-type bypass capacitors, and slug-tuned adjustable capacitors were used. At first, standard methods of coil construction were tried. These standard methods could not produce coupled coils with small enough values of stray capacitance. A novel method of spiral winding was used to give close coupling with small values of stray capacitance. The flat coils were made by a photoresistant etching process.

The coupling was adjusted by changing the spacing between the two etched boards. The two main advantages of using these etched coils were: 1) Once the first coil had been constructed, it could be

easily copied to provide all the coils needed for the fourteen identical sections constructed. 2) All copies of the original coil were identical. (This advantage of ensuring identical coupled coils for each section was very valuable when the problem of tuning was considered.)

The prefilter coils were constructed in the standard solenoidal form since a shunt capacitance was required anyway for one coil, and the other coil, because of its small value, could be wound with a small value of stray capacitance.

E. TUNING AND ADJUSTMENTS

This section describes the methods used to adjust the components to the values determined in the previous section on design and construction. The general procedure followed was to first adjust the elements to their specified values individually, and then to make final adjustments after the elements were mounted on the chassis. The second step in this procedure, the in-circuit adjustment, was necessary because of stray capacitance and inductance which could not be easily measured.

The prefilter was the easiest part of the matched filter to adjust. The coils were set to the calculated values using the RX meter. The capacitors were set with the capacitance bridge. The elements were assembled, a 2-ns pulse was applied, and the output pulse was observed on a Hewlett Packard Model 185B sampling scope. The only adjustment required was to compensate for the shunt

capacitance across the output of the prefilter by slightly decreasing the value of the final trimmer capacitor.

The tuning of the grid and plate lines proved to be a more difficult task. Four adjustments were necessary for each of the twenty-one sections, which meant that 84 parameters, all of which interacted, determined the response of the delay lines. To obtain the correct setting of the capacitors, the stray capacitance associated with the tube and socket were measured. The trimmers were then set on the capacitance bridge so that the combination of stray and trimmer capacitance was equal to the calculated value. The capacitors across the coupled coils were also set to less than the calculated values in order to compensate for the unavoidable stray capacitance. In fact, for the plate line, no additional capacitors were required across the plate-line coils.

The coils were the most troublesome elements to adjust. It was important that the inductance and coupling be as calculated. It was even more important that all of the cascaded constant-resistance sections have identical coils. Fortunately, the method of etching the flat coils ensured that they were identical. For the flat coils, the coupling was determined by the spacing between and alignment of the coil boards. It was found that coupling is quite sensitive to alignment. The T equivalent circuit of Figure 18 can be used to explain the method of adjusting the coupling of the coils. First, the inductance of the individual coil was checked. The total inductance to be expected with the coils coupled is given by $L_T = 2(1 - k)L$. Since the coupling

coefficient is negative, the total inductance of the two coils when coupled is greater than twice the individual inductance. After all of the forty-two pairs of coils were adjusted in this manner, they were carefully mounted on the chassis and connected together.

Two methods of in-circuit tuning were used. First, the resonant frequencies were set to the values calculated below using a grid-dip meter. Finally, the trimmers were adjusted for the desired pulse shape.

The following method of tuning, based on resonant frequency measurements, allowed the stray elements to be considered as part of the network (which they certainly are). Consider the balanced lattice used as a basis for the design of the delay line shown in Figure 25. The resonant frequencies to be considered are given by:

$$f_0 = f_{0_1} = \frac{1}{2\pi\sqrt{L_1 C_1}} = f_{0_2} = \frac{1}{2\pi\sqrt{L_2 C_2}} = \frac{\sqrt{a_0}}{2\pi} \quad . \tag{33}$$

This measurement ensured that the combination of stray capacitance and trimmer capacitance was the value specified to resonate with the known values of inductance. These two resonant frequencies could be measured with a grid-dip meter with only minor changes of the circuit. If the connection to the capacitor $2C_2$ was opened at d, a circuit was obtained with a resonant frequency given by:

$$f_0 = \frac{1}{2\pi\sqrt{C_1 L(1-k)}} = \frac{1}{2\pi\sqrt{C_1 L_1}} = \frac{\sqrt{a_0}}{2\pi} \quad , \tag{34}$$

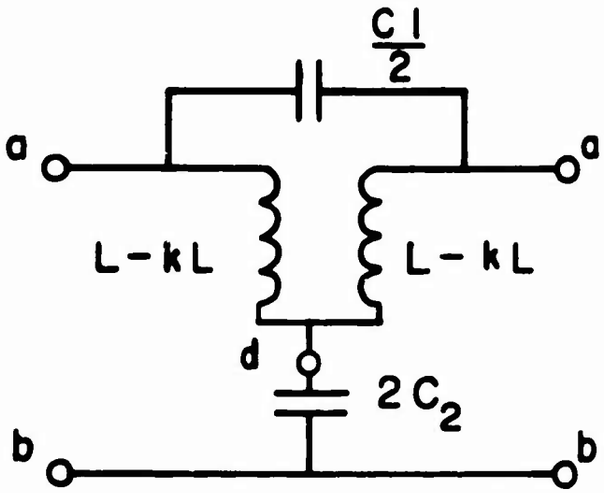

$$L = \frac{1}{2}\left[\frac{1}{a_1} + \frac{a_1}{a_o}\right]$$

$$k = \frac{\left[\frac{1}{a_1} - \frac{a_1}{a_o}\right]}{\left[\frac{1}{a_1} + \frac{a_1}{a_o}\right]}$$

FIGURE 25. Unbalanced Lattice Network.

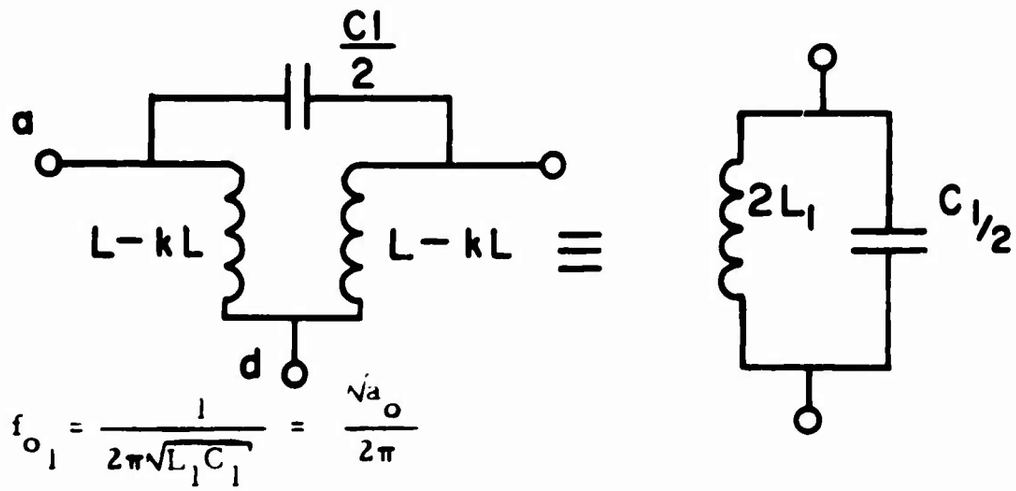

$$f_{o_1} = \frac{1}{2\pi\sqrt{L_1 C_1}} = \frac{\sqrt{a_o}}{2\pi}$$

FIGURE 26. Determination of f_{0_1}.

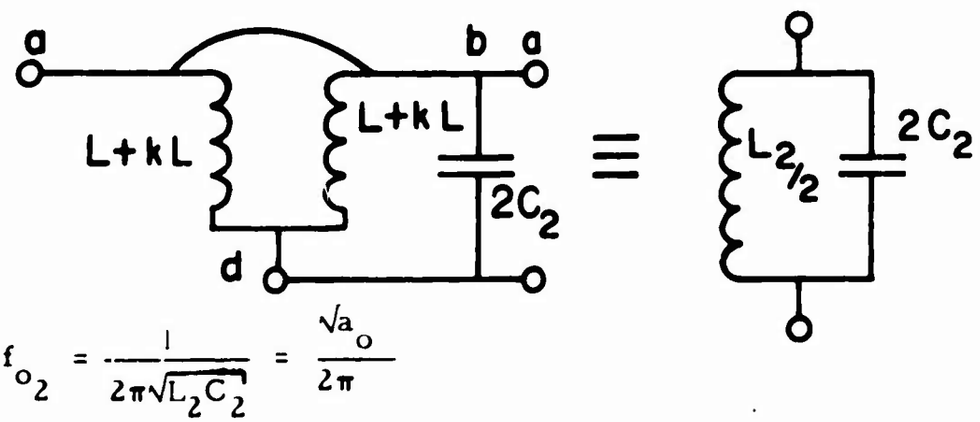

$$f_{o_2} = \frac{1}{2\pi\sqrt{L_2 C_2}} = \frac{\sqrt{a_o}}{2\pi}$$

FIGURE 27. Determination of f_{0_2}.

as shown in Figure 26. If the points a are connected to the points b effectively short-circuiting C 1/2, a circuit results with a resonant frequency of

$$f_0 = \frac{1}{2\pi\sqrt{C_2 kL}} = \frac{1}{2\pi\sqrt{L_2 C_2}} = \frac{\sqrt{a_0}}{2\pi} \quad , \qquad (35)$$

as shown in Figure 27. Thus with two simple measurements, the capacitance of the trimmer capacitors and the stray capacitance can be combined to give the specified value.

Difficulty was encountered with this method. It was difficult to obtain a zero impedance path (short) in the 50-Mc/s range with this method of construction. However, the method of resonant frequencies did serve to provide a good setting for C 1/2.

The method of adjustment which finally produced the best results was based on observation of the time response of the network. This method involves adjusting one section of the delay line at a time to give the specified delay without distorting the pulse. The first step was to make these connections: the previously adjusted prefilter to one section of the grid line, the grid line to the corresponding tube, and the tube to one section of the plate line. As shown in Figure 28, the grid- and plate-line sections were terminated with their characteristic resistance: 100 ohms for the grid line, and 400 ohms for the plate line.

The output of this one section of plate line was observed on the sampling scope. The trimmer capacitors of the grid and plate line

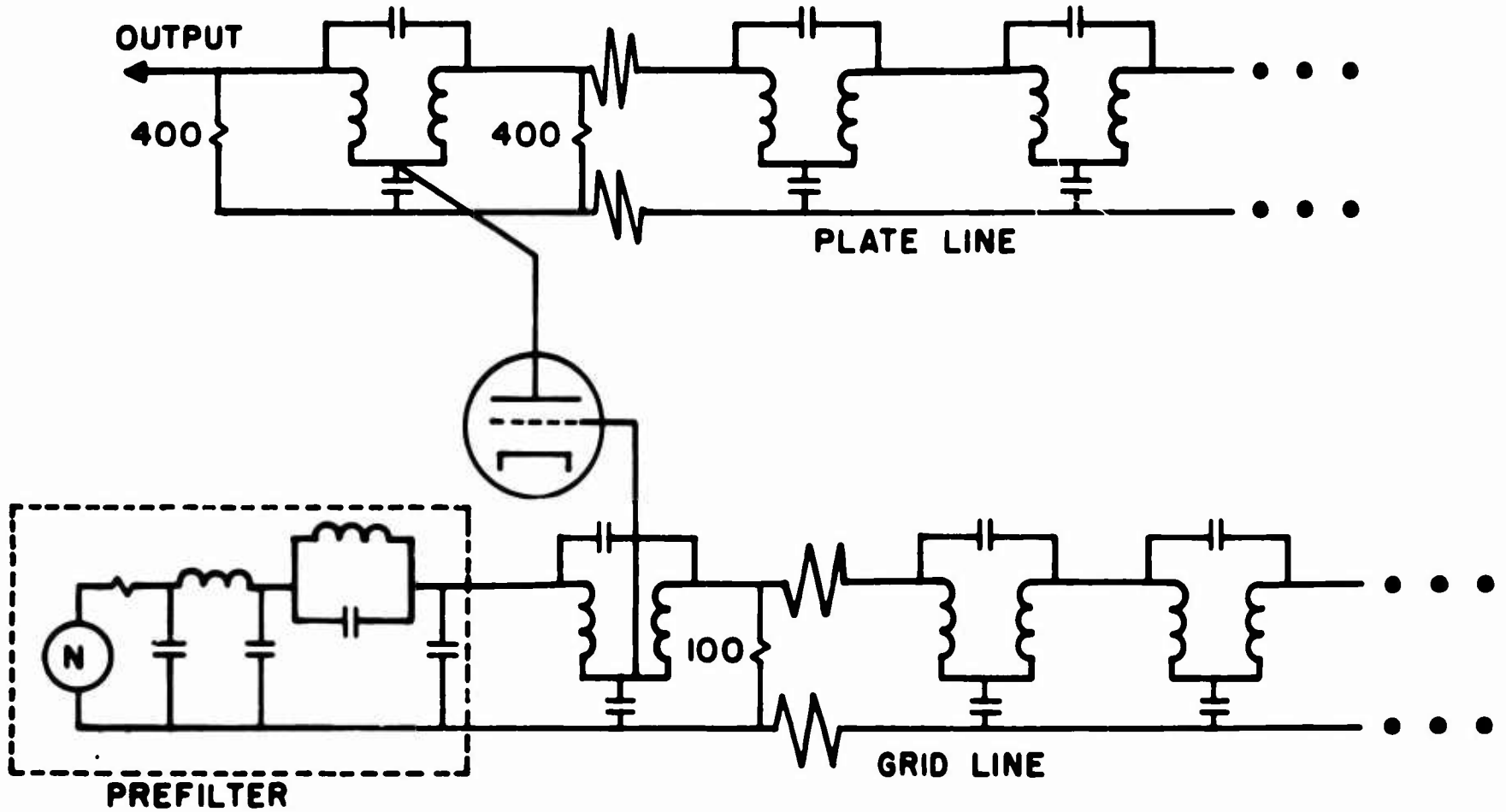

FIGURE 28. Method of Step-by-Step Tuning.

were then adjusted to give the desired pulse shape. Next, a second section of grid line was added, after moving the termination resistor from the first section to the second. The pulse output of the one plate-line section was distorted by this step because the second section did not have exactly the constant-resistance input impedance desired. Minor adjustment of the trimmer capacitors restored the pulse output to the desired shape.

The next step was to add a second section of plate line, moving the 400-ohm termination from the first section to the second. This plate section was then adjusted so that its impedance appeared as a 400-ohm resistance. Next, the tube was moved from the first position to the second. A plug simulating tube capacitance was inserted in the first socket. The pulse output of the first section was now a delayed, slightly distorted version of the prefilter output.

The second sections of grid and plate line were given final adjustments to give the specified delay of 20 ns without distortion. A third section of grid line was then added, and the procedure was repeated until all seven sections of grid and plate line were adjusted. The other grid line was tuned in a similar manner.

Finally, all seven tubes were connected to give the desired code. The output was the sum of seven replicas of the prefilter output with various amplitudes. The gain of each tube was then adjusted so that the output consisted of three positive pulses, followed by two negative pulses, followed by one positive and one negative pulse – all of the same amplitude. This seven-pulse code is shown in Figure 3.

IV. EXPERIMENTAL RESULTS

The first part of the matched filter to be tested was the prefilter. A Hewlett Packard Model 185B sampling oscilloscope was used to observe the output of the prefilter. The synchronizing pulse from the oscilloscope was used to trigger a pulse generator which provided pulse of 2-ns duration. This pulse was roughly one-tenth the duration of the impulse response proved to be a good approximation to an impulse. The prefilter was terminated with the parallel combination of the gridline input impedance and the input impedance of the inverting amplifier as shown in Figure 6. A photograph of the prefilter output is given in Figure 29.

Next, a measurement was made to determine if the delay through one signal path (combined effect of one section of grid line and one section of plate line) was actually equal to one-half of the pulse width at half-amplitude. When the delay was equal to half the pulse width, the sum of two pulses should have had a flat top, i.e. no peak or trough should have appeared. Figure 30 shows a multiple exposure which confirms that the correct relation between pulse width and delay was obtained. Three exposures are shown: the individual pulse, the individual pulse delayed, and the sum of these two pulses.

This multiple exposure technique was also used to show how three pulses add (Figure 31). Some of the ripple at the top was caused by the overshoot or ringing of the individual pulses. Another multiple exposure photograph (Figure 32) shows the sum of seven pulses

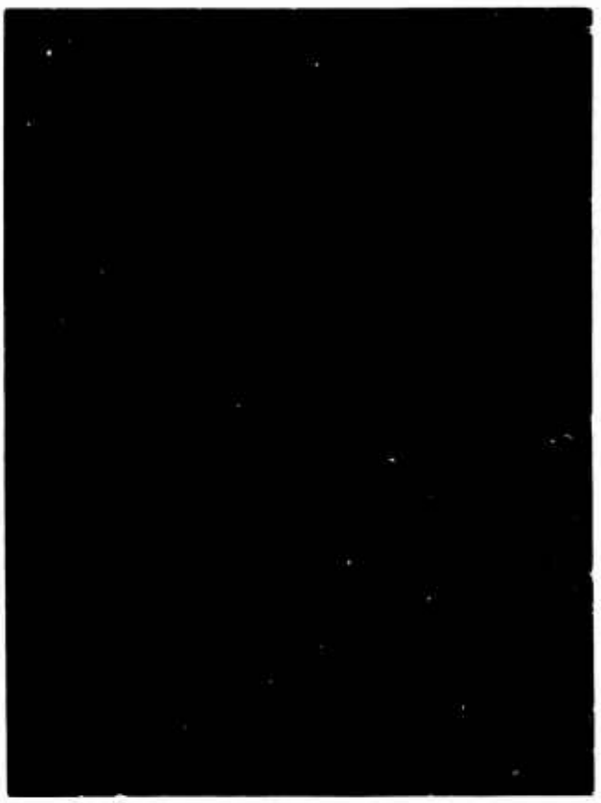

FIGURE 29. Prefilter Output.

FIGURE 30. Summation of Two Pulses.

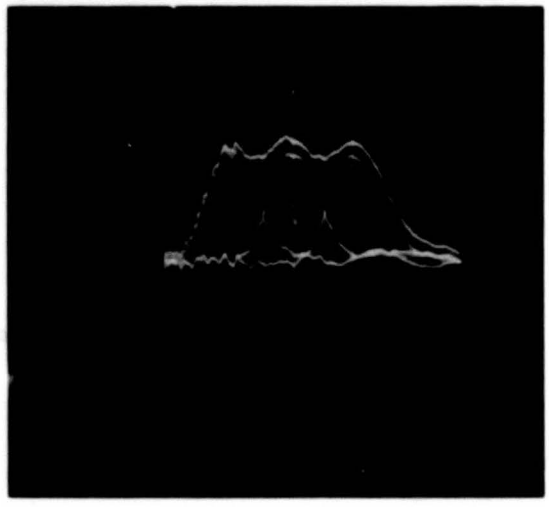

FIGURE 31. Summation of Three Pulses.

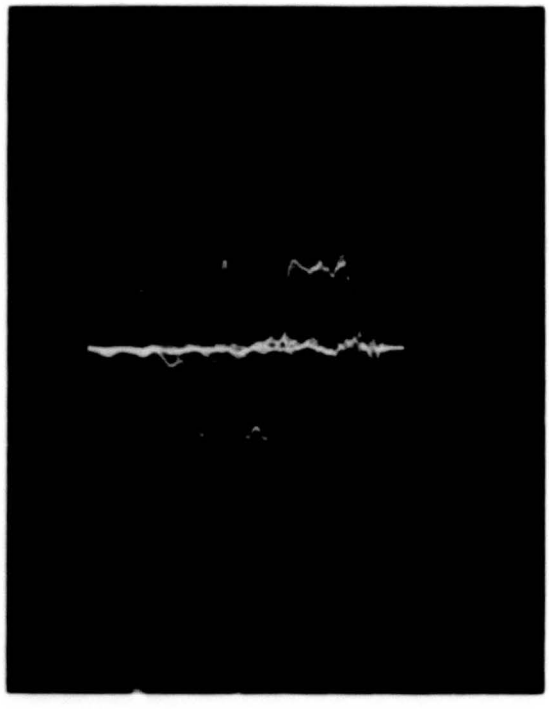

FIGURE 32. Formation of Seven-Pulse Code.

combined to produce the desired code. This figure, while cluttered, is instructive. For example, it shows that while the combination of seven pulses appears to be made up of the sum of pulses with the same absolute value of amplitude, the individual pulses do not all have the same amplitude. Slight adjustments in gain coefficients were necessary to compensate for the overshoot of adjacent pulses.

Figure 33 shows the output of the entire matched filter. The ripple at the top of the signal could be decreased by using a slightly wider prefilter output pulse. The ringing at the end of the signal is the sum of the overshoot of all seven pulses. This problem of ringing, which was caused mostly by the impossibility of taking into account all stray effects, is a major limitation in the design of wide-band structures to produce longer codes. Two identical matched filters were connected in cascade to produce a fourteen-pulse code, as shown in Figure 34. This output could have been improved slightly by more careful tuning.

To show the performance of the combination of signal generator and matched filter, the two identical networks were arranged as shown in Figure 35. The impulse response of network I, which is used as the input to network II, is shown at the top of Figure 36. The impulse response of network II, which is simply the time reverse of the input to network II, is shown at the bottom. The output of the matched filter (network II) has a large central peak, as shown in the center of Figure 36. The ratio of this peak to the amplitude of the ripple on either side should theoretically be 7:1, if the prefilter output were a square

FIGURE 33. Impulse Response of Matched Filter.

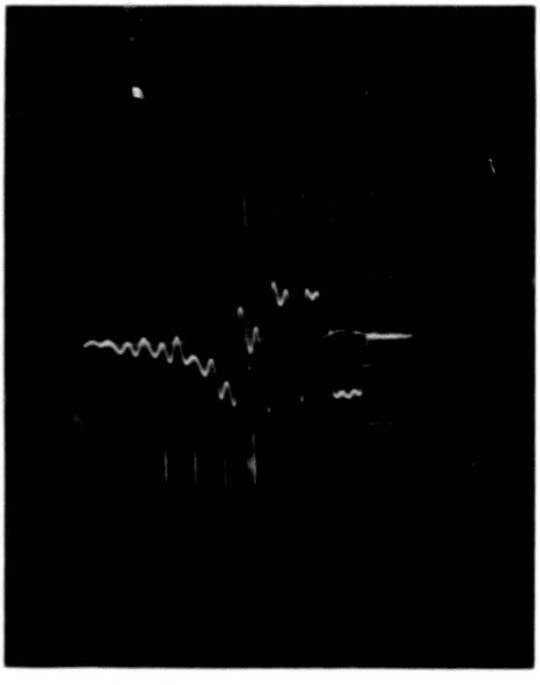

FIGURE 34. Fourteen-Pulse Code.

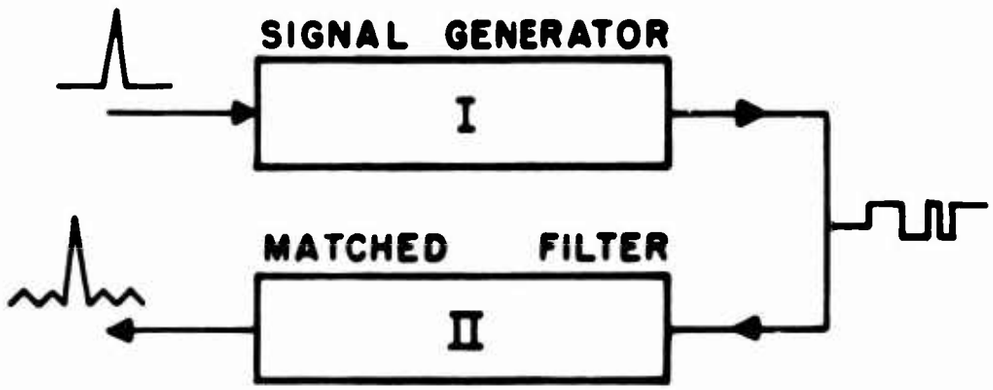

FIGURE 35. Stretching, Then Compressing Pulse.

pulse and the delay line were ideal. The actual ratio attained, as measured from Figure 36, was slightly greater than 4:1. The use of the rounded prefilter output pulse with a normalized autocorrelation function of .7475 should theoretically give a ratio of 5.2:1. The further reduction in ratio of peak to ripple may be accounted for by the increased ripple resulting from errors in the grid and plate lines.

Figure 37 shows the improvement in signal-to-noise ratio which was obtained experimentally (the output is at the top). For the same rms noise level at input and output, the output peak should be about twice that of the input. The measured improvement was less than expected, which may be explained by the fact that the bandwidth of the noise generator used was only about half that of the matched filter. If a noise generator with bandwidth greater than that of the matched

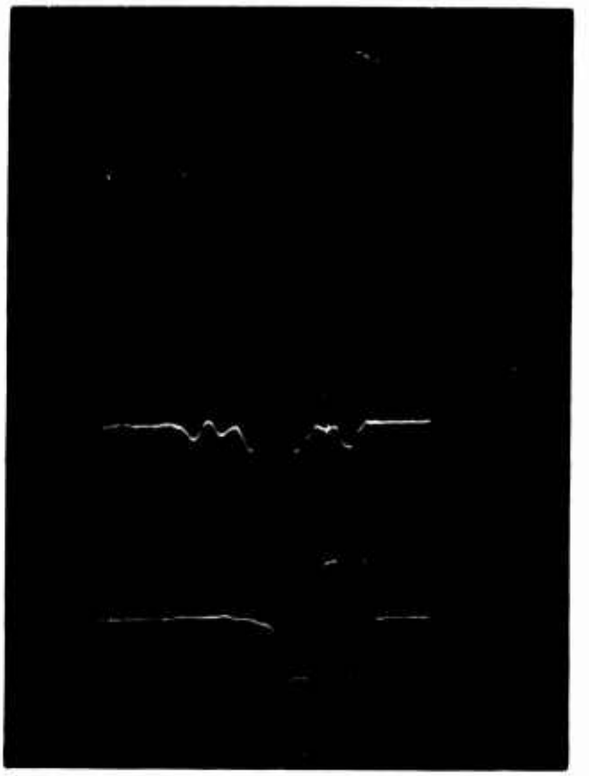

a) Output of Signal Generator

b) Output of Matched Filter

c) Impulse Response of Matched Filter

FIGURE 36. Performance of Matched Filter

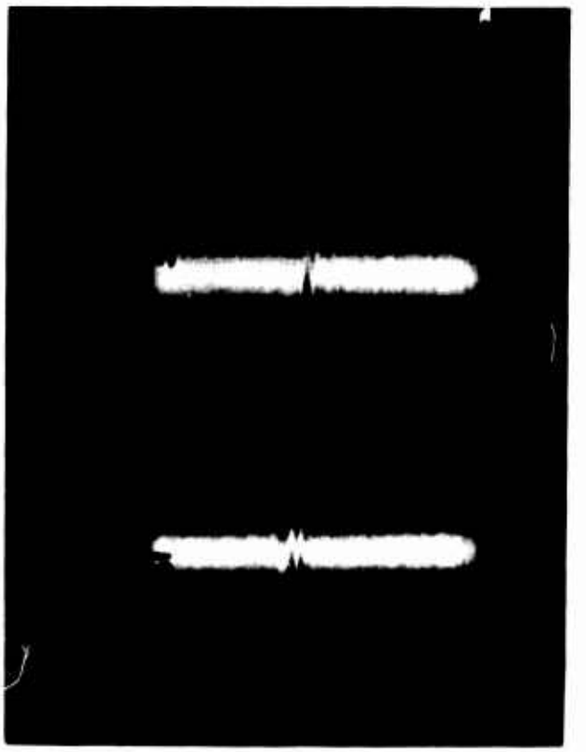

FIGURE 37 Performance of Matched Filter with Noise.

filter were used, the noise could be considered "white" over the band of interest, and the signal-to-noise ratio improvement would be greater.

Figure 38 compares the performance of a three-pulse code with that of a seven-pulse code. For the same pulse heights (peak power-limited case), the code of 7 should give a peak output signal about $7/3$, or 1.5 times that for the code of 3.

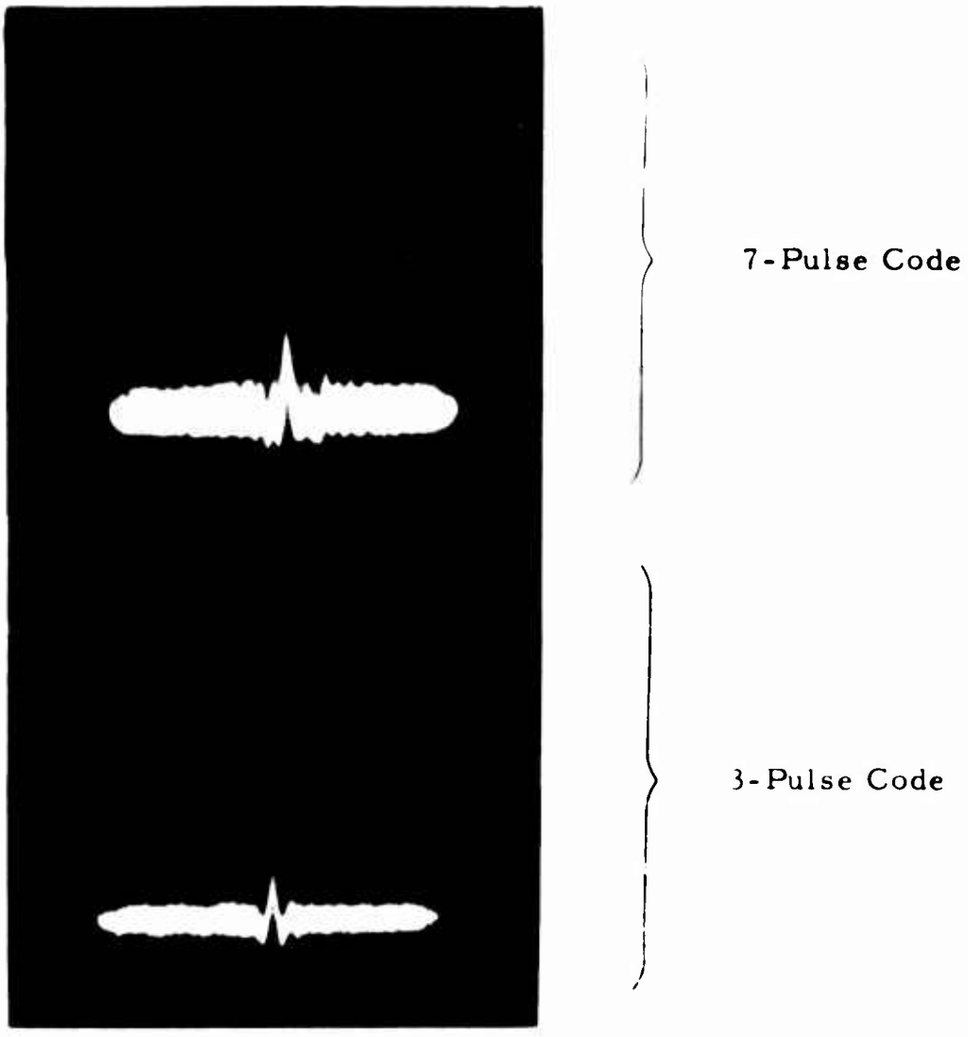

FIGURE 38. Comparison of the Performance of Matched Filters with Noise.

V. CONCLUSION AND RECOMMENDATION FOR FURTHER STUDY

This research has involved the synthesis, construction, and measurement of a signal generator and matched filter. Lumped element networks were used in a link structure with a 50 Mc/s bandwidth. Measurements have shown that this particular method of construction may be extended to slightly higher frequencies (on the order of 100 Mc/s) and slightly longer codes (up to twice the length used). However, the mostly practical limitations encountered with this method prevent its use for the construction of networks with very large time bandwidth products and lead to the following suggestions for further study.

Since both theoretical problems and practical problems were encountered, recommendations are made for both kinds of study. The major theoretical topic suggested for further study is that of time-domain approximation. How can one design a delay line so as to minimize the difference between the input signal described as $f(t)$ and the delayed version of this signal $f(t - \tau)$? Another problem area has to do with the present requirement for coupled coils. Construction would be much easier if ladder networks could be used for the grid and plate lines. How can one design a ladder network with a specified relation between the input function of time and n output time functions?

The practical problems suggested for study concern the method of construction. The idea of printing or etching the individual sections of grid and plate line should lead to the development of better methods

of producing identical sections. Perhaps the entire network including capacitors could be printed or etched. A method of reducing the sensitivity of the over-all network to the stray capacitance and inductance associated with individual components would be to increase the order or number of elements used for each section of the grid and plate lines. If the sensitivity to the individual element values were reduced sufficiently, the time-consuming procedure of in-circuit tuning could perhaps be eliminated by careful adjustment of each element before assembly of the entire network.

VI. REFERENCES

1. G. L. Turin, "An Introduction to Matched Filters," IRE Trans., IT-6 (June 1960), pp. 311-329.

2. R. S. Kalluri, "Link Amplifier as a Coded-Pulse Generator and Matched Filter," Research Report EE 491, Cornell Univ., April 1961.

3. D. W. Lytle, "Experimental Study of Tapped Delay Line Filters," Tech. Rep. No. 361-3, Stanford Univ., July 1956.

4. H. S. McGaughan, "The Link Amplifier as a Coded Pulse Generator and Matched Filter," in Research Report EE 467, Cornell Univ., February 1960, pp. 132-147.

5. N. DeClaris, H. S. McGaughan, R. Kalluri, "Synthesis of Signal Generators and Matched Filters," Proc. of the Nat. Elec. Conf., 17 (1961), pp. 111-125.

6 H. W. Schüssler, "Design of a Link-Type Matched Filter," in Research Report EE 557, Cornell Univ., Feb. 1963, pp. 68-83.

7. H. W. Schüssler, "About the Design of a Matched Filter," unpublished memorandum, Cornell University, School of Elec. Eng.

8. E. A. Guillemin, Synthesis of Passive Networks, New York: Wiley and Sons, 1957, pp. 194-205.

9. J. Jess, and H. W. Schüssler, "Über Filter mit gunstigem Einschwing verhalten," Archiv der Elektrischen Übertragung, 16 (1962), pp 117-128

10. K. Ganapathy, "A Wide-Band Voltage Variable Amplifier," Research Report EE 490, Cornell Univ., April 1961.